Lithos 114 (2010) 337–352

Contents lists available at ScienceDirect

Lithos

journal homepage: www.elsevier.com/locate/lithos

Geochemistry and petrogenesis of late Miocene granitoids, Cyclades, southern Aegean: Nature of source components

C. Stouraiti [a,*], P. Mitropoulos [a], J. Tarney [b], B. Barreiro [c], A.M. McGrath [b], E. Baltatzis [d]

[a] Department of Geochemistry and Economic Geology, National and Kapodistrian University of Athens, Panepistimioupolis, Ano Ilisia 15784 Athens, Greece
[b] Department of Geology, University of Leicester, Leicester LE1 7RH, UK
[c] NERC Isotope Geoscience Laboratory, Kinglsey Dunham Centre, Keyworth, Nottingham NG12 5GG, UK
[d] Department of Mineralogy and Petrology, National and Kapodistrian University of Athens, Panepistimioupolis, Ano Ilisia 15784 Athens, Greece

ARTICLE INFO

Article history:
Received 15 June 2009
Accepted 29 September 2009
Available online 19 October 2009

Keywords:
Cyclades granites
I-type
S-type
Dehydration melting
Sr–Nd isotopes

ABSTRACT

Neogene igneous activity in the Aegean region comprised both extrusive volcanism and intrusive granitoid plutonism. Granitoid plutonism in the Cyclades was established in the mid-Miocene period and lasted until late Miocene (18 to 9 Ma). The timing of granitoid intrusion was associated with the initiation of extensional tectonics in the Aegean. These intrusions form a broad belt about 200 km long running from the west (Lavrium and Serifos) to the eastern Aegean. Both S-type and I-type granitoids are present, the former generally being emplaced earlier than the I-types (~15 to 8.3 Ma). Major and trace element variations reveal that three end-member components are involved in the granitoids, but the proportions of these vary in the different plutons. Initial isotopic compositions of all the granitoids are typical of crust-derived magmas from heterogeneous metasedimentary sources (I-type: $^{87}Sr/^{86}Sr = 0.7091–0.712$, $\varepsilon_{Nd} = -6.4$ to -10.4; S-type: 0.710–0715, $\varepsilon_{Nd} = -7.5$ to -10.1). Three end-member sources have been identified: 1) One end-member appears to be a metasedimentary biotite-gneiss (greywacke-type) such as that forming the metamorphic core complexes (Naxos and Paros); this is a dominant (but not the only) component in the S-types. 2a) Major, trace element and Sr–Nd isotopic composition correlations of the S-type granitoids with basement gneiss require an extra source of Sr and Ca, having lower initial $^{87}Sr/^{86}Sr$ indicating a more depleted metasedimentary source at depth, due to possible interaction, of metamorphic fluids with marbles and amphibolites and infiltration through the gneissic units, at mid-crustal levels. 2b) A possible second end-member could be the marble component, as indicated by the buffered values of the Initial Sr isotopic ratios. Major element variation of the mafic microgranular (quartz diorites and tonalites) enclaves are compatible with dehydration melting of a mafic source similar to the amphibolites (island arc tholeiites) at medium pressure (~8 kb) conditions. 3) Amphibolite is another end-member which may contribute mostly to the source of the younger intrusions, along the western flank of the arc.

1. Introduction

Partial melting within the crust is a widely accepted model for the production of some, if not most, granite magmas (White et al., 2003). Dehydration melting, involving the breakdown of hydrous minerals, is inferred to be the main melt-producing process in the crust (e.g. Thompson, 1982; Vielzeuf and Holloway, 1988; Brown, 1994; Gardien et al., 1999; White et al., 2003). It is considered that partial melting is a result of melt-forming reactions as temperatures and possibly pressure increase (e.g. Wolf and Wyllie, 1991; Wyllie and Wolf, 1993; Skjerlie and Johnston, 1996; White et al., 2003). Metapelite melting can occur by dehydration melting of muscovite at about 700 °C (at ~5 kb), followed by biotite at 750 °C, whereas dehydration melting of hornblende in amphibolites appears to require temperatures near 900 °C in a pressure range from 5 to 10 kb (e.g. Wolf and Wyllie, 1991; Rushmer, 1991; Wyllie and Wolf, 1993).

However, in terms of source fertility, greywacke-type metasediments contain the appropriate components (plagioclase, quartz, biotite, amphibole and possibly epidote) to form a granitic liquid, under dehydration melting conditions (Skjerlie and Johnston, 1996). Melting of metagreywacke produces larger volumes of granitic melt than melting of metapelites as a result of its Na_2O content and the increased Fe/Mg of biotite (Patiño-Douce and Beard, 1995; Thompson, 1996). Some examples of hornblende-bearing felsic igneous rocks have been interpreted as being products of anatexis of biotite + plagioclase + quartz gneisses (Gardien et al., 2000). Experimental studies on a wide range of synthetic and natural biotite + plagioclase + quartz assemblages have

* Corresponding author. Tel.: +30 210 8643015x8029307; Mobile: +30 6945372965.
E-mail addresses: ch.stouraiti@dpers.minenv.gr, ch.stouraiti@hotmail.com (C. Stouraiti).

0024-4937/$ – see front matter © 2009 Elsevier B.V. All rights reserved.
doi:10.1016/j.lithos.2009.09.010

shown that amphibole forms during partial melting of a previous amphibole-free assemblage; however external H_2O is required to stabilize amphibole during anatexis of a biotite + plagioclase + quartz assemblage (Gardien et al., 2000; Johnston and Wyllie, 1988).

In the Attic–Cycladic Massif, metasedimentary gneisses are often interlayered with basaltic and other metavolcanic rocks (amphibolites), marbles and other metasediments in a regional metamorphic terrain. The Cycladic Blueschist Unit underwent HP–LT regional metamorphism (M1) between 55 and 40 Ma ago (Andriessen et al., 1979; Altherr et al., 1982; Wijbrans and McDougall, 1988; Bröcker et al., 1993; Baldwin and Lister, 1994, 1998), followed by greenschist to amphibolite (M2) facies metamorphism dated from 25 to 16 Ma (Andriessen et al., 1979; Altherr et al., 1982; Wijbrans and McDougall, 1988; Bröcker et al., 1993). On several Cycladic islands these two metamorphic units were intruded by granitoids.

In contrast to most other Cycladic islands, the Miocene Barrovian-type metamorphism reached anatectic conditions on Naxos (670 ± 50 °C and 5–7 kb) (Jansen and Schuiling, 1976; Buick and Holland, 1989) and created an onion-shaped migmatite dome in the central part of the island. It has been proposed that the recorded rapid uplift triggered decompression melting in the gneiss dome of Naxos at progressively deeper structural levels, with the final intrusion of I-type granodiorites at about 12.5 Ma, based on zircon dating (Henjes-Kunst et al., 1988).

The source of specific Cycladic granitoids still remains to be clarified. Previously proposed petrogenetic models for the formation of the Miocene Cyclades I-type granites have been formulated mostly in terms of two component mixing, either, between mantle-derived magmas (arc-type basalt) and/or, mantle-derived igneous rock (i.e. obducted ophiolites) and upper crust end-members (Juteau et al., 1986; Altherr et al., 1988). Recently, it has been suggested that both I- and S-type granitoids originated by dehydration melting of metaluminous upper crustal sources (Altherr and Siebel, 2002). U–Pb systematics of zircon populations suggests a high proportion of assimilated crustal material in these magmas (Juteau et al., 1986; Altherr and Siebel, 2002).

In the present paper we extend our investigation of the involvement of the different basement rocks of the Attic–Cycladic Massif, in the generation of the I- and S-type plutons. We present new Rb–Sr, Sm–Nd isotope data as well as precise chemical data (major and trace elements) for all the Cycladic granitoids and for a variety of basement rocks from the Cycladic islands (Paros, Naxos and Serifos) and are evaluated along with existing isotope data. Because Sr and Nd isotopic compositions alone cannot distinguish between the different hypotheses for the petrogenesis of the igneous rocks in a given region, an overall evaluation of geochemical, mineralogic, regional tectonics and field observation data is attempted.

2. Regional setting and field relationships

In the central Aegean, the Attic–Cycladic Massif forms a belt of metamorphic rocks exhumed along low-angle detachments (Lister et al., 1984). The polyphase tectonometamorphic evolution of this massif began with an Eocene high-pressure/low-temperature metamorphism evidenced by blueschist to eclogite facies (Andriessen et al., 1979; Wijbrans and McDougall, 1988; Buick and Holland, 1989; Baltatzis, 1996; Avigad et al., 1998; Keay and Lister, 2002).

The high-pressure/low-temperature metamorphism was overprinted by a Miocene medium pressure/medium temperature event evidenced by a greenschist to amphibolite-facies locally reaching partial melting conditions (Jansen and Schuiling, 1976; Andriessen et al., 1979; Altherr et al., 1982; Buick and Holland, 1989; Keay, 1998; Keay et al., 2001; Keay and Lister, 2002) (Fig. 1). The *P–T–t* evolution of the Cyclades metamorphic belt is best documented on the island of Naxos (Buick and Holland, 1989).

The Attic–Cycladic Massif is a structurally complex pile of tectonic units separated by faults. It is possible to distinguish at least two major tectonic units (Andriessen et al., 1987; Ring et al., 1999b; Brichau, 2004). The island of Naxos in the Attic–Cycladic Massif displays the most complete structural cross section of the Cyclades (van der Maar and Jansen, 1983; Andriessen et al., 1987; Henjes-Kunst et al., 1988; Buick and Holland, 1989) where three tectonic units have been distinguished. The upper tectonic unit, structurally above the detachment, is composed of low-grade marble, schists and serpentinites that are unconformably overlain by dominantly detrital Cenozoic sediments. The middle and lower units are composed of high-grade metamorphic rocks located below the detachment. The middle unit is composed of a sequence of schists (at the bottom) and marbles (at the top) sequence containing mafic and ultramafic boudins (Jansen and Schuiling, 1976). The lower unit is made of felsic metasedimentary gneisses and marbles. The lower unit gneisses become migmatites and occupy the core of dome of the Metamorphic Core Complex of Naxos and Paros, mantled by metamorphic rocks of the middle unit.

On Naxos, a structural section through the middle and lower units is marked by a medium pressure/medium temperature metamorphic gradient ranging from greenschist facies to amphibolite facies reaching partial melting (10 kb, 750 °C) as demonstrated by migmatites exposed in the centre of the dome (Jansen and Schuiling, 1976; Buick and Holland, 1989; Avigad and Garfunkel, 1991; Duchêne et al., 2006). High pressure/low temperature metamorphism is only represented by relics of blueschist facies metamorphic minerals, such as Na-amphibole and jadeite (10 kb, 350 °C), in the south of the island.

Based on isotopic age studies, the gneisses from the basal units of the central Cyclades islands (Naxos, Sikinos, and Ios) have been described by several authors as pre-Alpine basement, consisting of metamorphosed Variscan granites (Andriessen et al., 1987; Pe-Piper et al., 1997; Reischmann, 1998). However, more recent work on the petrological and geochemical character of the core gneisses of Naxos migmatite dome (cf. Buick, 1988) and the provenance of their zircons (Keay, 1998) suggest the core may be comprised of Mesozoic metasediments or S-type granites, interlayered with rare thin slivers of Variscan orthogneiss, making the use of the term “Basement” of questionable value (Keay et al., 2001).

Miocene extension was accompanied by the emplacement of I- and S-type granites which intruded the detachments and/or affected syn-extensional shearing (Altherr et al., 1982, 1988; Henjes-Kunst et al., 1988; Lee and Lister, 1992; Pe-Piper et al., 1997; Bröcker and Franz, 1998; Pe-Piper, 2000; Altherr and Siebel, 2002; Pe-Piper et al., 2002; Iglseder et al., 2008; Brichau et al., 2008). Most of the Cycladic granites are assigned to the I-type category (Altherr et al., 1982, 1988; Altherr and Siebel, 2002), some of which constitute composite intrusions (Serifos and Ikaria). S-type granites (two-mica fine grained leucogranites) are mostly associated with zones of migmatisation in the high-grade metasedimentary gneisses of the lower unit, with typical examples that of the Metamorphic Core Complexes of Naxos and Paros.

3. Petrography of Cyclades granitoids and basement rocks

3.1. I-type granitoids

Most Cycladic plutons conform to the I-type category of Chappell and White (1974, 1992) (cf. Altherr et al., 1982, 1988; Altherr and Siebel, 2002) (Fig. 1). The petrography of these rocks has been established in previous studies (Altherr et al., 1982; Salemink, 1980; Altherr et al., 1988; Pe-Piper, 2000; Altherr and Siebel, 2002; Pe-Piper et al., 2002; Skarpelis et al., 2008). They contain, hornblende, titanite, allanite, biotite and therefore are metaluminous in composition (lacking primary muscovite, garnet and monazite). Details of the sample description for representative granite samples, are given in Table 1.

Commonly the I-type granites consist of compositionally different rock-types ranging from granite, granodiorite to minor tonalite in composition (Altherr et al., 1982, 1988). Mafic microgranular enclaves are found in all the I-type granitoids but in variable abundance in each pluton. Their compositions vary from diorite, to quartz diorite to tonalite (Altherr et al., 1982; Stouraiti, 1995; Pe-Piper et al., 2002) and are

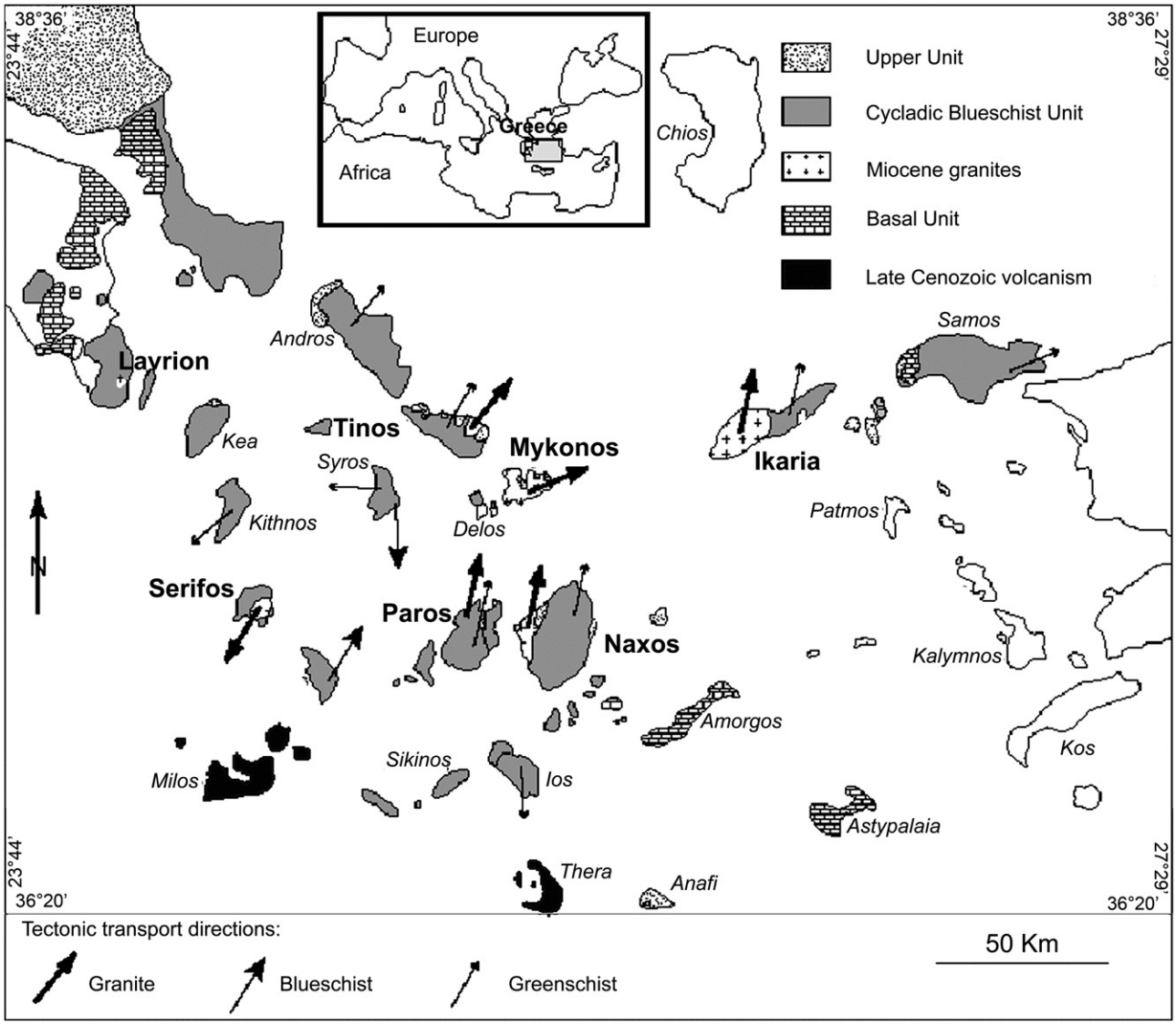

Fig. 1. Simplified geologic map of the Cycladic zone with the locations of granite intrusions and orientations of tectonic transport of different rock types: granites, greenschist facies and blueschist facies (map modified from Dürr et al., 1978; Altherr et al., 1982; Avigad and Garfunkel, 1991; Forster and Lister, 1999; Ring et al., 1999; Brichau, 2004).

generally they more common at the margin of the plutons. The more felsic I-type granitoids such as Tinos and Ikaria granites tend to have fewer, or no, mafic enclaves. These features reveal the complexity in the intrusive processes responsible for the compositional heterogeneity in the granitoids (Altherr et al., 1988).

3.2. S-type granites

Granites of this category form: a) dykes and sheets of fine grained leucogranites, b) veins of pegmatites and aplites often bearing tourmaline ± garnet, c) separate intrusive bodies (e.g., the Paros Kolimbithres biotite granite, and the Ikaria eastern intrusion). S-types are more common in the central Cyclades islands (Tinos, Paros, Naxos and Ikaria, (Fig. 1). Precise dating of pluton emplacement has proved difficult because of resetting of mineral geochronological clocks as a result of metamorphism and deformation (Henjes-Kunst et al., 1988), however the ages ranges (18 to 11.5 Ma) from the classic work of Altherr et al. (1982) are accepted by most workers in the area.

The mineralogical composition of these granites have been well documented by previous authors (Altherr et al., 1982; Pe-Piper et al., 1997; Pe-Piper, 2000; Altherr and Siebel, 2002; Pe-Piper et al., 2002). They typically contain primary muscovite, Al-rich biotite, plagioclase, alkali-feldspar ± garnet). Additional accessory phases in these granites are tourmaline, apatite, zircon, magnetite, ilmenite and yellow allanite (Altherr et al., 1982).

On Naxos, Barrovian-type metamorphism reached anatectic conditions, creating an elongated migmatite dome. S-type granites were intruded during the waning stages of migmatisation (15.4 to 11.3 ± 02 Ma, Keay et al., 2001) and form dykes within the migmatitic gneiss. S-type granites and pegmatite dikes on Paros intrude the lower unit lithologies (gneisses/amphibolites/amhibolite schists/marbles) unit but show close spatial association with the metasedimentary gneisses. Field data demonstrate that gneisses are tectonically homogenized but still broad bands of more psammitic and more pelitic type can be distinguished. Evidence for local melting occurs near the pelite horizons, as seen by multiple generations of synextensional pegmatite veins formation (e.g., Monasteri peninsula).

In this study, samples from S-type granitoids from Paros, Naxos, Tinos and Ikaria were investigated (Tables 1 and 2).

3.3. Basement rocks

Gneisses comprise a major part of the structurally lower tectonic units in the Attic–Cycladic Massif. They become very homogenized

Table 1
List of samples studied, locality, ages, rock type and classification.

Region	Age Ma (intrusion age)*	Locality	Sampl. no.	Rock type	Classification
Lavrion — S. Attica	8.3	Plaka	LA-2	Granodiorite	I-type
			LA-3	Granodiorite	I-type
Serifos isl.	~9	Livadhi	SER-1	Granodiorite (margin, foliated)	I-type
		Livadhi	SER-26	Granodiorite (outer, with abundant mafic enclave)	I-type
		Troulos	SER-56	Granodiorite (inner)	I-type
		Cape Khalara	SER-30	Qtz diorite (enclave)	I-type
Mykonos isl.	~11	Port	MYK-1	Bit-Granite	I-type
			MYK-2	Hbl-Bit-granodiorite	I-type
			MYK-3	Hbl-Bit-granodiorite	I-type
Paros isl.	(12.4–11.5)	Kolimbithres	P-5	Bit granite	S-type
		Kolimbithres	PA-12	Bit granite	S-type
		Kolimbithres	P-14	Bit granite	S-type
		Naousa	PA-13	Bit granodiorite	S/I type
		Naoussa	PR-7	Bit granodiorite	S/I type
		Naousa	PA-15	Leucogranite	S-type
		Monasteri	PA-4	Leucogranite	S-type
		Monasteri	PA-9	Tourmaline + garnet pegmatite vein	S-type
Naxos isl.	14–12	Mikri Vigla	NX-1	Hbl-Bit granodiorite	I-type
		Mikri Vigla	NX-2	Hbl-Bit granodiorite	I-type
		Mikri Vigla	NX-4	Hbl-Bit granodiorite	I-type
		Mikri Vigla	NX-5	Hbl-Bit granodiorite	I-type
		Glinados	NX-8	Hbl-Bit granodiorite	I-type
		Glinados	NX-10	Bit-Hbl granodiorite	I-type
		Vivlos	NX-12	Granodiorite	I-type
Migmatite dome	24–16	Kinidaros	NX-14	Migmatite (with amphibolitic inclusions)	S-type
		Kinidaros	NX-16G	Granite	I-type
		Naxos port	NX-18	Granodiorite	I-type
Tinos isl.	16–14	Krokos	TI-1	Bit-Msc granite	S-type
		Krokos	TI-2	Bit granite	I-type
		Falatados	TI-3	Bit-Hbl granite	I-type
		Falatados	TI-4	Bit-Hbl granite	I-type
		Pyrgos	TI-6	Bit-Msc granite	S-type
Ikaria isl.	~8–10	Western intrusion	IKR-1	Bit granite	I-type
	18 – 9.4	Eastern intrusion	IKR-2	Bit-Msc granite	S-type
Basement: gneisses, amphibolites					
Naxos		Melanes	NX-17	Migmatised gneiss — core of dome	
Paros		Naoussa	PR-6	Biotite Gneiss	Metagreywacke
Serifos		Spathi cape	SER93-52	Leucocratic band, layered mylonitic gneiss	
		Spathi cape	SER93-50	Biotite rich band, mylonitic gneiss	Metagreywacke
Naxos	–	Kinidaros	NX-13	Amphibolite inclusion in migmatitic gneiss	Metabasic
Serifos		Pyrgos	SER93-20	Amphibolite within greenschists unit	Metabasalt (calc alkaline)

(migmatitic) as metamorphic grade increases as shown in the center of the metamorphic complexes of Naxos and Paros (northern part of Paros) and metasediments become more common at the periphery of domes (McGrath, 1999). Field data and petrological investigations of Naxos, Paros and Serifos gneissic rocks and metasedimentary schists indicate that metagreywacke is the predominant rock-type over meta-pelite, semipelites and arkoses, with intercalations of quartzite and marble up to a few meters thick (Stouraiti, 1995; McGrath, 1999).

In the middle and upper tectonic units of the Attic–Cycladic Massif there are alternations of marbles and schists. Within these units mafic metavolcanic rocks (amphibolites) and serpentinites commonly occur. These rocks may represent the metamorphosed parts of disrupted ophiolite complexes, or the volcanic fraction of the arc crust. These rocks are enclosed as bands or conformable lenses. In the high-grade gneisses of migmatite domes on Naxos and Paros, amphibolite blocks display high ductility and are isoclinally folded and boudinaged. In the central part of the Naxos migmatite dome, greywacke gneiss, marble and amphibolites become complexly folded and contorted; amphibolite rocks become coarse-grained hornblende-rich inclusions within metasediments and marbles.

4. Samples and analytical methods

To determine the geochemical characteristics of the different granitic intrusions 35 samples, from the representative lithological types of each pluton, were selected for study. Additionally, 6 samples from representative lithological types from the surrounding country rocks from central Cyclades (Paros and Naxos) and western Cyclades (Serifos) islands, were selected for bulk rock and mineralogical analyses, in order to investigate the contribution of different basement rocks in the generation of the granites. Comparison of the geochemical data of the metasedimentary gneisses from this study, with available data on Paros basement gneisses (McGrath, 1999) was carried out, in order to investigate the different rock types within the gneiss unit. The selection of samples from basement rocks was based on evaluation of field evidence, geochemical and mineralogical data (e.g. Serifos, Stouraiti, 1995; Paros and Naxos, McGrath, 1999) and available literature data.

Samples were jaw crushed and ground to a fine flour in an agate mortar prior to analysis by XRF techniques. Major elements were determined on fused discs using Rh anode excitation, and the trace elements Sc, V, Cr, Ni, Zn, Ga, Rb, Sr, Y, Zr, Nb, La, Ce, Nd and Ba on pressed powder briquettes using either Rh or W excitation on the Phillips PW1600 X-ray fluorescence spectrometer at Leicester University (for techniques see Marsh et al., 1983).

Radiogenic isotope ratios and Nd and Sm concentrations were analysed at the NERC Isotope Geosciences Laboratory. Sr and Nd were separated from dissolutions of 150–400 mg powdered samples using ultra-clean reagents and conventional cation exchange columns. Procedural blanks for Sr, Nd and Sm averaged 500 pg, 126 pg, and 341 pg respectively during the period of analysis. Sr isotopic

compositions were measured in static mode on a Finnigan MAT 262 multicollector mass spectrometer whilst Nd isotopic composition was measured both in static mode on the Finnigan and in dynamic mode on a VG 354 multicollector mass spectrometer. $^{87}Sr/^{86}Sr$ was normalised to $^{86}Sr/^{88}Sr = 0.1194$, $^{143}Nd/^{144}Nd$ was normalised to $^{146}Nd/^{144}Nd = 0.7219$. Within-run precision for Sr and Nd isotope ratios, expressed as one standard error of the mean, was always better than 10 ppm of the measured ratio, i.e. 0.000007 and 0.000005 for $^{87}Sr/^{86}Sr$ and $^{143}Nd/^{144}Nd$ respectively.

Results for isotope standards during the period of these measurements were:

NBS 987 $^{87}Sr/^{86}Sr = 0.710195 \pm 0.000011$ ($n = 10$),
Seawater $^{87}Sr/^{86}Sr = 0.709117 \pm 0.000007$ ($n = 12$),
Johnson–Matthey Nd $^{143}Nd/^{144}Nd = 0.511127 \pm 0.000007$ ($n = 15$) and
La Jolla Nd $^{143}Nd/^{144}Nd = 0.511851 \pm 0.000008$ on the VG 354 ($n = 10$) and 0.511871 ± 0.000007 ($n = 9$) on the Finnigan (all errors: one standard deviation).

Internal errors on individual measurements were always much smaller than the standard reproducibility reported here and therefore the ability to reproduce the standards should be taken as the limiting factor in interpreting the uncertainty of any given analysis.

5. Results

5.1. Major elements

Major and trace element compositions of representative samples of the Cyclades granitoids are listed in Table 2. On the alkali-silica classification diagram (Fig. 2, after Cox et al., 1979), Cyclades I-type granitoids span the field of normal alkalinity of granodiorite and granite, and the S-type granitoids plot in the field of granite. Normative values of quartz, alkali feldspar and plagioclase are plotted in Fig. 3, showing again that S-types are typically granites and I-types span the fields of granodiorite and granite. Mafic enclaves from the Serifos pluton (Stouraiti, 1995, unpubl. data) plot in the field of quartz–diorite and represent the most mafic magmatic component (available in the present study) (Figs. 2 and 3). The peraluminosity index (molar $Al_2O_3/CaO + Na_2O + K_2O$, or A/CNK) varies from 0.8 to 1.1 for the I-type granites, and characterizes their metaluminous to weakly peraluminous bulk composition (Fig. 4). The S-type granitoids are weakly peraluminous ranging from, 1 (Paros Bi-Granite) to 1.15 (Paros Bi-Granodiorite). Their A/CNK values show no correlation with the SiO_2 content, possibly reflecting heterogeneity within their source protolith. The weak peraluminosity of the S-type granites is expressed also in their modal composition by the absence of aluminosilicate minerals.

Representative local basement gneiss samples from different islands (Paros, Naxos and Serifos) display a similar variation in A/CNK index as the S-type group, (Table 2). Pegmatite/aplite veins intruding this type of gneiss (biotite-rich) contain tourmaline and garnet, and are considered to be partial hydrous melts of the gneissic host rocks.

In most Harker variation diagrams (Fig. 5) major oxides in the Cyclades granitoids display broad linear correlation and partially overlapping fields between S- and I-types (Fig. 5). I-type Granodiorites (Serifos–Lavrion–Naxos) have higher MgO contents (2.6–1.0 wt.%) than granites (Mykonos–Tinos–Ikaria), in which MgO content varies from 1.7 to 0.4%. The enclaves from the Serifos intrusive complex display distinctly higher MgO (4.9–3.55 wt.%) contents — as expected from their mafic modal mineralogy (Fig. 5). However they define a continuum with the rest of the Serifos intrusion and the other of the I-type granitoids, showing a broad linear variation which may indicate mixing relationships between a mafic and felsic end-member. The variation in CaO abundance with increasing SiO_2 clearly separates I-type (4.5–1.6 wt.%) and S-type granitoids (2.9–0.8 wt.%), the latter obviously being less calcic (Fig. 5). Similarly Fe_2O_3 displays a broad correlation with SiO_2 and separates the two types of granitoids (I-type ranging from 4.3 to 1.5 wt.% and S-type from 2.3 to 0.5 wt.%). P_2O_5 show a bimodal variation: Serifos composite intrusion (enclaves–tonalite–granodiorite) and Lavrion granodiorite display an almost constant (buffered) abundance of P_2O_5 (0.13–0.08 wt.%), indicating the buffering effect of apatite. All the other granitoids (I- and S-) display a well correlated variation of P_2O_5 (0.2–0.03 wt.%) with SiO_2. Analyses of the metasedimentary gneisses and schists show significant variation in P_2O_5.

Leucogranites and S-type granites with less biotite tend to have significantly higher Al_2O_3/TiO_2 ratios than the more biotite-rich (more mafic) granites (Fig. 6). This is well displayed in the Paros S-type granites: the mean value of the Al_2O_3/TiO_2 ratio of (two-mica) leucogranites is significantly higher (183–497) than biotite granite (51–55) and biotite granodiorite (27–47).

5.2. Trace elements

Trace element variations with SiO_2 do not distinguish between the I-type and the S-type granitoids (Fig. 7). Primitive mantle-normalised multi-element diagrams can be employed to emphasize compositional variations amongst the Cyclades granites (Figs. 8 and 9). If all Cyclades granitoids magmas were derived from similar sources, the observed compositional differences could be a result of variations in (1) the degree of partial melting, (2) the relative amounts of melt and restite in the magmas, and (3) restite mineralogy caused by variable *P–T* conditions of partial melting and magma segregation (Altherr and Siebel, 2002).

The multi-element patterns of all the Cyclades granitoids are remarkably similar and show the following features: (a) general enrichment in the Large Ion Lithophile (LIL) elements (Rb, Ba, K, Th and Sr) relative to the Light Rare Earth Elements (LREE) and High Field Strength (HFS) elements (Nb, Zr, P, Ti and Y), (b) marked negative anomalies for P and Ti, but variable negative anomalies for Nb, and (c) small or no negative anomaly for Sr and depressed LREE abundances (relative to the LILE). Some of these chemical characteristics show spatial zonation: i.e. the granitoids from the central part of the Cyclades (Naxos (-Tinos) and Mykonos; Fig. 1), exhibit more extreme trace element features: a) the highest LIL element enrichment pattern (K, Rb and Th), b) higher Sr–Ba concentrations (Mykonos), and c) higher LEE and P abundances relative to all the other Cyclades granitoids. Ikaria biotite–granite shows similar but less extreme features relative to Naxos. These characteristics are shared by the most "mafic" compositions of the S-type granitoids (e.g. Paros biotite granodiorite, Fig. 9). A qualitative comparison of both granite types with the trace element patterns of the abundant biotite gneisses (metagreywacke) in the basal units of the Attic–Cycladic Massif, show remarkable similarities in most trace element pattern for LIL elements (Rb, Ba and K) and LREE, and similar negative anomalies for Nb, P and Ti, indicating that this type of the metasedimentary basement rock contributes to a large extent (if not being the only source) to the generation of both I and S-type Cyclades granitoids. However, there is a significant Sr enrichment in most I-type granitoids, up to 2.5 times in the I-type (Mykonos), relative to the biotite–gneisses. Sr enrichment is correlated with high Ba. These chemical characteristics may reflect heterogeneities within the metasedimentary source that cannot be traced at the present level of exposure of the basement units.

Assuming a biotite-gneiss as starting composition for Cyclades granitoids, plagioclase as a major carrier for Sr and Ba should contribute to a large extent either as a reactant phase or as a restite mineral in the I-type group and the more "mafic" compositions of the S-type (Paros biotite–granodiorite). Based on melting experiments in biotite–plagioclase–quartz gneisses (Mogk, 1992; Gardien et al., 1999), it has been shown that K-feldspar-rich granitic melts can be formed according to the incongruent melting reaction of biotite in the assemblage biotite + plagioclase (I) + quartz, under fluid-absent (dehydration) or fluid present

Table 2
Representative whole-rock analyses (XRF, oxides in wt.%) of Cyclades granites and basement rocks.

Cyclades granites																		
Sampl.	LA-2	LA-3	SER-1	SER-56	SER-30	SER-2a	MYK-1	MYK-3	NX-10	NX-14	NX-16G	NX-18	NX-1 N	NX-5	NX-8	PA-4	PA-9	PA-12	PA-13
SiO_2	70.6	71.2	68.6	64.5	58.8	61.1	69.5	67.2	70.4	76.5	69.7	69.5	71.4	68.7	68.8	75.40	74.04	72.35	67.91
TiO_2	0.45	0.44	0.70	0.60	0.65	0.83	0.61	0.72	0.50	0.11	0.61	0.63	0.41	0.63	0.63	0.03	0.06	0.28	0.57
Al_2O_3	14.6	14.5	15.5	16.3	16.4	17.0	15.1	15.1	14.4	13.6	14.2	14.5	14.0	14.9	14.5	14.93	14.87	15.42	16.70
Fe_2O_3	3.01	2.64	3.60	4.30	5.00	5.00	2.83	4.33	2.78	0.92	3.27	3.23	2.35	3.46	3.25	0.53	0.63	1.72	3.02
MnO	0.02	0.01	0.09	0.05	0.07	0.13	0.04	0.07	0.05	0.03	0.05	0.05	0.05	0.05	0.06	0.08	0.01	0.03	0.03
MgO	0.95	0.89	1.55	2.53	4.89	3.55	1.20	1.70	1.32	0.25	1.33	1.32	1.04	1.69	1.34	0.08	0.16	0.37	0.86
CaO	2.95	3.03	4.05	5.06	6.56	5.54	3.24	4.44	2.98	1.05	3.00	3.57	2.69	3.59	3.13	1.21	1.10	1.94	2.74
Na_2O	2.75	2.60	3.40	3.15	2.97	3.47	2.50	2.98	2.69	2.90	2.74	2.59	2.87	2.60	2.71	4.24	3.26	3.60	3.51
K_2O	3.70	3.70	2.72	2.62	3.10	3.05	4.52	3.45	4.61	5.00	4.21	3.87	4.36	4.15	4.39	3.87	5.24	4.19	3.84
P_2O_5	0.11	0.11	0.11	0.11	0.12	0.13	0.16	0.18	0.14	0.03	0.18	0.15	0.12	0.18	0.20	0.04	0.05	0.09	0.17
LOI	0.60	0.42	0.62	0.90	0.77	0.67	0.40	0.34	0.38	0.22	0.30	0.40	0.63	0.61	0.54	0.30	0.28	0.39	0.54
Total	99.7	99.5	100.9	100.2	100.4	100.50	100.1	100.5	100.2	100.6	99.6	99.8	99.9	100.5	99.5	100.31	99.41	99.98	99.34
Sc	78	3	16	14	22	36	11	11	7	4	10	8	7	12	12	6	5	8	9
V	50	47	64	93	115	97	36	43	36	5	38	31	32	47	45	10	10	17	24
Cr	10	4	61	6	247	30	9	16	32	3	21	11	9	25	25	8	<1	24	2
Co	42	35	8	11	15	13	37	38	39	36	38	46	35	40	30	<2	<2	3	6
Ni	<1	<1	2	8	12	7	7	9	10	<1	<1	<1	17	10	5	<1	<1	0	1
Cu		2	6	4	6	8	2	7	3	<1	1	<2	2	7	5	<2	<2	<2	1
Zn	16	9	109	82	86	129	44	73	40	20	51	46	36	54	49	17	21	34	50
Ga	18	18	15	16	17	16	20	24	20	22	21	18	20	20	20	20	20	22	23
Rb	110	100	81	70	78	99	172	206	213	283	237	184	235	189	219	214	207	214	159
Sr	414	425	299	371	404	287	519	370	410	95	359	412	333	455	404	68	159	242	383
Y	30	27	27	24	31	41	40	27	26	39	28	44	28	31	33	28	36	11	15
Zr	223	220	220	163	161	203	296	357	212	80	238	233	193	257	232	57	47	169	318
Nb	17	16	15	9	5	15	20	21	21	24	27	30	25	26	25	8	24	9	9
Ba	745	790	607	644	480	689	1035	447	562	182	484	564	469	601	604	87	438	552	976
La	29	28	23	21	18	23	36	36	29	19	30	34	23	40	33	10	10	17	35
Ce	49	51	41	38	38	49	69	74	56	41	58	74	41	75	69	18	10	32	74
Nd	24	21	20	19	27	26	24	28	25	19	25	34	15	27	26	8	2	9	24
Th	14	14	7	7	5	4	11	14	10	20	16	18	16	23	17	8	13	14	19
A/CNK	1.07	1.05	0.98	0.95	0.82	0.90	1.02	0.91	0.97	1.10	0.98	0.97	0.98	0.98	0.98	1.12	1.14	1.11	1.12

conditions, and the amount of fluid controls the temperature at which the melting reaction takes place. Such reactions produce plagioclase and hornblende as well as granitic melt (Gardien et al., 1999), although hornblende stability requires small amounts of (2–4 wt.%) water to be added to the system.

Serifos and Lavrion granitoids, on the western flank of the arc, display more mafic major element compositions and also the least fractionated trace element patterns (Fig. 5), despite the large variation in silica content of this pluton, 64 to 72 wt.% (Stouraiti, 1995). Serifos–Lavrion also demonstrates a slightly different trend from the rest of Cyclades granitoids, with regard to Rb, K/Rb, Zr, and Ba, as depicted in the flat LILE pattern. They show a narrow enrichment in most LILE, a distinct Th depletion, and higher K/Rb relative to the other I-type granites (Fig. 7b). However, they lack the Sr (negative) anomalies and show only a small Ba anomaly, relative to the other granites. These features can be attributed to either a) different *P–T* conditions of partial melting of a common source where plagioclase dissolves in the melt (carrier of high Ba–Sr) and hornblende remains as residual phase, accounting for the low Y and high K/Rb, or b) infiltration of a Sr-rich metamorphic fluid after interaction with marble at the biotite-gneiss/marble interface, during high-grade metamorphism (M2 phase) and partial melting in mid-crustal levels. Alternatively, if a magma mixing model is considered, then Serifos–Lavrion granitoids could be hybrid, containing a larger fraction from a mafic source (possibly amphibolite) or from the mafic magma.

The negative Ti and Nb anomalies in the Cyclades granitoids are similar to those of the metasedimentary gneisses (Fig. 9) and are ultimately attributed to titanite being stable in the source during partial melting. It has been suggested that granodioritic–tonalitic melts can be formed by partial melting of migmatitic biotite–plagioclase paragneisses under low *P*, high *T* according to the reaction, biotite + plagioclase + quartz = hornblende + sphene + anorthite-rich plagioclase + (K-feldspar + anorthite-poor plagioclase + H_2O + quartz) melt (Gardien et al., 1999). There is an unusual Nb enrichment in the Tinos and Naxos S-type granites relative to biotite-gneiss composition (average Paros gneiss and Serifos) and much higher than average continental crust (~19 ppm: Wedepohl, 1995). In the Tinos S-type granite, Altherr et al. (1982) documented the existence of columbite, $(Fe,Mn)(Nb,Ta)_2O_6$, and ilmenite which reflects the unusual enrichment of Nb in this granite due, possibly, to late stage fractionation.

5.3. Sr and Nd isotopes of granites and basement rocks

New Sr and Nd isotope analyses are reported in Table 3, and displayed in Fig. 10, S-type granites display significant heterogeneity in their initial $^{87}Sr/^{86}Sr$ ratios from 0.71003 (Tinos) to 0.71587 (Ikaria). One leucogranite (PA15) sample within the biotite-gneiss (from Paros basement) displays extremely high initial $^{87}Sr/^{86}Sr$ (0.76224) ratio which could be attributed to major fractionation of the Rb/Sr ratio of this sample. The I-type granites have a narrower variation in their initial $^{87}Sr/^{86}Sr$ ratios, ranging from 0.70909 (Serifos) to 0.71277 (Ikaria), and partially overlap with the variation of the S-type granites, yet heading towards distinctly lower initial $^{87}Sr/^{86}Sr$ ratios (Fig. 10). Metasedimentary (gneiss and schists) country rocks from Paros basement (McGrath, 1999, unpubl.) have initial $^{87}Sr/^{86}Sr$ ratios ranging from 0.714975 to 0.723871, whereas Paros (Kolombithres) biotite–granite, which represents the more voluminous S-type intrusion in the area and hosted by the metasedimentary gneisses, tends to show distinctly less radiogenic initial $^{87}Sr/^{86}Sr$ ranging from 0.711519 to 0.71184 similar to the I-type granites from the central Cyclades (Tinos and Mykonos). This feature indicates that, in terms of Sr isotopic compositions, the source for the Paros biotite–granite and for most of the S-type group (except Ikaria)

Granites												Basement rocks - Gneisses						- Amphibolites	
PR-7	PR-3	PR-4	P-14	PA-15	TI-1	TI-3	TI-4	TI-6	IKR-1	IKR-2	IKR-3	NX-17	PR-6	SER93-52	SER93-50	SER92-28	Average Paros (n=21)	SER93-20	NX-13
70.7	71.2	68.5	70.44	78.04	76.2	71.1	72.1	73.8	75.0	73.3	74.8	78.17	71.907	78.8	71.1	69.2	70.6	48.4	46.8
0.48	0.33	0.60	0.31	0.07	0.11	0.44	0.43	0.20	0.27	0.25	0.22	0.05	0.485	0.11	0.64	0.399	0.48	1.15	2.2
15.5	15.6	16.2	15.83	12.87	13.3	14.5	14.2	13.7	12.7	14.6	13.3	11.86	14.647	11.9	13.6	15.8	14.7	19	15.3
2.62	2.25	3.37	1.94	0.71	1.05	2.63	2.65	1.58	1.80	1.49	1.52	1.12	3.221	1.41	4.25	3.4	3.3	10.8	13.28
0.02	0.03	0.33	0.04	0.02	0.07	0.05	0.04	0.07	0.03	0.02	0.04	0.04	0.05	0	0.06	0.09	0.06	0.17	0.18
0.79	0.70	1.07	0.37	0.08	0.27	0.98	0.97	0.61	0.71	0.65	0.45	0.21	1.04	0.12	1.7	0.8	1.10	3.34	6.35
2.60	2.08	2.94	2.27	0.86	1.13	2.98	2.77	2.03	1.59	1.73	1.71	0.64	1.467	0.8	3.52	2.26	1.53	12.24	10.82
3.07	4.25	3.24	4.47	3.24	3.44	3.49	2.81	3.18	2.60	3.55	2.69	2.81	3.369	4.13	3.27	5.16	3.64	3.14	2.38
4.21	2.56	3.43	4.15	4.36	4.30	3.89	3.42	3.78	4.27	3.73	4.48	4.63	3.031	2.47	1.53	3.026	3.52	1.11	1.97
0.14	0.11	0.18	0.09	0.03	0.05	0.11	0.10	0.06	0.07	0.10	0.05	0.03	0.194	0.023	0.1	0.077	0.191	0.17	0.21
0.48	0.65	0.52	0.51	0.44	0.34	0.36	0.40	0.49	0.33	0.34	0.34	0.7	0.92	0.25	0.5	0.32	0.85	0.4	0.63
100.16	99.82	99.58	99.90	100.27	100.3	100.5	99.9	99.5	99.4	99.7	99.6	100.26	99.411	100.013	100.3	100.5	99.97	99.92	100.2
6	3	6	6	11	3	10	6	7	1	4	4	4.4	8.7	**5**	17	16	8.5	28	37
21	20	20	13	8	8	34	27	17	18	25	13	9	42.5	16.0	99	63	41	268	271
<1	<1	<1	4	1	7	6	6	5	4	5	9	3	9.5	1.80	43	47	23	35	130
33	43	42	2	<2	39	46	42	45	37	37	58	44	6.3	0.3	12	6	8.5	24	57
<1	<1	1	0	0	2	3	<1	1	4	3	<1	<1	3.5	<1	8	0	5	23	70
<1	<1	4	<2	<2	<2	1	<1	12	<2	<2	<2	<2	<2	<4	5	10	4	16	32
49	60	67	43	39	23	38	37	24	33	28	24	46	71.8	15.00	25	34	61	55	166
19	23	24	22	15	20	17	18	20	24	18	17	18	20.4	11.00	15	15	20	20	22
170	127	151	190	164	317	158	169	276	196	179	232	184	101.4	54.00	54	95	123	43	80
367	254	412	253	43	74	310	302	228	238	198	163	412	147.7	127	145	88	141	357	159
15	18	16	9	55	51	27	22	38	18	24	34	44	18.8	42	31	24	23	37	60
315	203	346	179	49	81	184	200	105	136	128	108	233	184.5	119	194	142	166	180	119
10	13	11	10	8	47	17	16	30	9	14	15	30	12.2	7	9	4	12.	8	26
992	422	875	552	110	143	526	500	506	436	292	305	564	659.6	522	287	345	692	203	130
34	21	31	21	13	11	19	19	14	18	24	19	33.8	25	47.6	21	20.7	23.2	16	30
62	42	59	37	33	24	34	40	24	34	44	33	74.3	47.3	74.5	39	38.2	47	39	43
23	18	19	12	15	11	12	17	8	12	20	13	34.1	21	32.4	25	17.7	17	23.7	31
20	13	17	11	9	22	13	10	17	10	17	18	18.2	10.9	15	8.3	11	11	1	4
1.09	1.16	1.13	0.99	1.11	1.08	0.95	1.07	1.05	1.08	1.12	1.08	1.10	1.28	1.09	1.02	1.00	1.17	0.67	0.60

and all the I-type group, is not the presently exposed level of gneisses but another end member which controls Sr isotopic variation in mid- or lower-crustal levels.

S-type granites have initial ε_{Nd} ranging from −7.5 to −10.1, whereas the respective values of I-type granites range from −6.3 to −9.3. Metasedimentary gneisses from Paros basement units have a remarkable heterogeneity in ε_{Nd} values ranging from −5.1 to −10.8 (average ε_{Nd} of 9 samples, −9) and ε_{Nd} of the Serifos gneiss samples range from −8.5 to −9.9.

Available Sr isotopic data from marbles in the Cyclades (Naxos marble, $^{87}Sr/^{86}Sr$: 0.708, Andriessen, 1978; Santorini marble, initial $^{87}Sr/^{86}Sr$: 0.708084, by Briqueu et al., 1986) show that the Sr isotopic ratios of marbles may set a lower limit to the initial Sr isotopic ratios of central southern Aegean granitoids. Any contribution from a mafic source could therefore be masked by metasomatic isotopic interchange between marble and amphibolite (sometimes also blueschists or eclogites), though trace element contributions may be more overt. Evidence of this isotopic interchange comes from amphibolite lenses (e.g. #Na-13) within the Naxos gneiss dome. This sample, age-corrected to the culmination of M2b at 16 Ma (Wijbrans and McDougall, 1988), has an unusually high initial $^{87}Sr/^{86}Sr$ ratio (0.7099) relative to its Nd isotopic composition ($\varepsilon_{Nd(t)}$ = −2.2), close to the Sr isotopic composition of Naxos marbles (Fig. 11). However, it is clear that Sr isotopes can be exchanged with much greater facility than Nd (cf. Lesher, 1990); the ε_{Nd} values of the amphibolites may be much closer to that of the mafic protolith.

6. Discussion

6.1. Petrogenesis of mafic enclaves

Comparisons of major element composition of the microgranular quartz–diorite–tonalite enclaves (Serifos) with experimental melt compositions from different metabasaltic sources show that their high MgO (up to 5 wt.%) and CaO (max. 7 wt.%) (Fig. 5), their metaluminous composition (Fig. 4) and their low Ti, are compatible with melt compositions from dehydration melting experiments at medium pressures, up to 8–10 kb, and a starting composition of island arc tholeiites (Rushmer, 1991).

Partial melting and crystallization experiments of quartz–amphibolite at 3–15 kb (Patiño-Douce and Beard, 1995) showed that dehydration-melting begins from T~850 °C (at P = 3 kb), and produces peraluminous granodioritic melts (SiO_2 > 70%) that coexist with clinopyroxene + orthopyroxene + plagioclase + quartz (± garnet, at P > 10 kb). Trace element determinations of suspected partial melts from metabasites showed that melts (generated at P = 8–10 kb, and T = 800–850 °C) are composite, having a restite component which dominates the HREE (depletion) and Sr (positive anomaly) and a melt component which dominates the incompatible elements, as seen in the tonalite–trondhjemite–granodiorite (TTG) gneiss suites (Storkey et al., 2005).

REE patterns of the Cyclades I-type granites are similar and show essentially unfractionated HREE patterns, with high $(La/Yb)_n$ and low $(Tb/Yb)_n$. (Pe-Piper et al., 1997; Altherr and Siebel, 2002; Skarpelis et al., 2008). These features are incompatible with substantial amounts of garnet either in the residue during partial melting and final re-equilibration or as part of the fractionating assemblage in the deep crust. The documented negative Ba (Figs. 8 and 9) and Eu anomalies in Cyclades granitoids indicate evolution of the I-type granites–granodiorites within the plagioclase (and K-feldspar) stability field. HREE depletion in the more felsic granites of Naxos and Mykonos would however be compatible with some late-stage crystal fractionation of garnet from the peraluminous granitic melts (Fig. 8).

Sr–Nd (and O) isotope compositions (Table 3, Fig. 10: Initial $^{87}Sr/^{86}Sr$ = 0.710, $\varepsilon_{Nd(t)}$; −7.2) of the mafic enclaves are equilibrated with

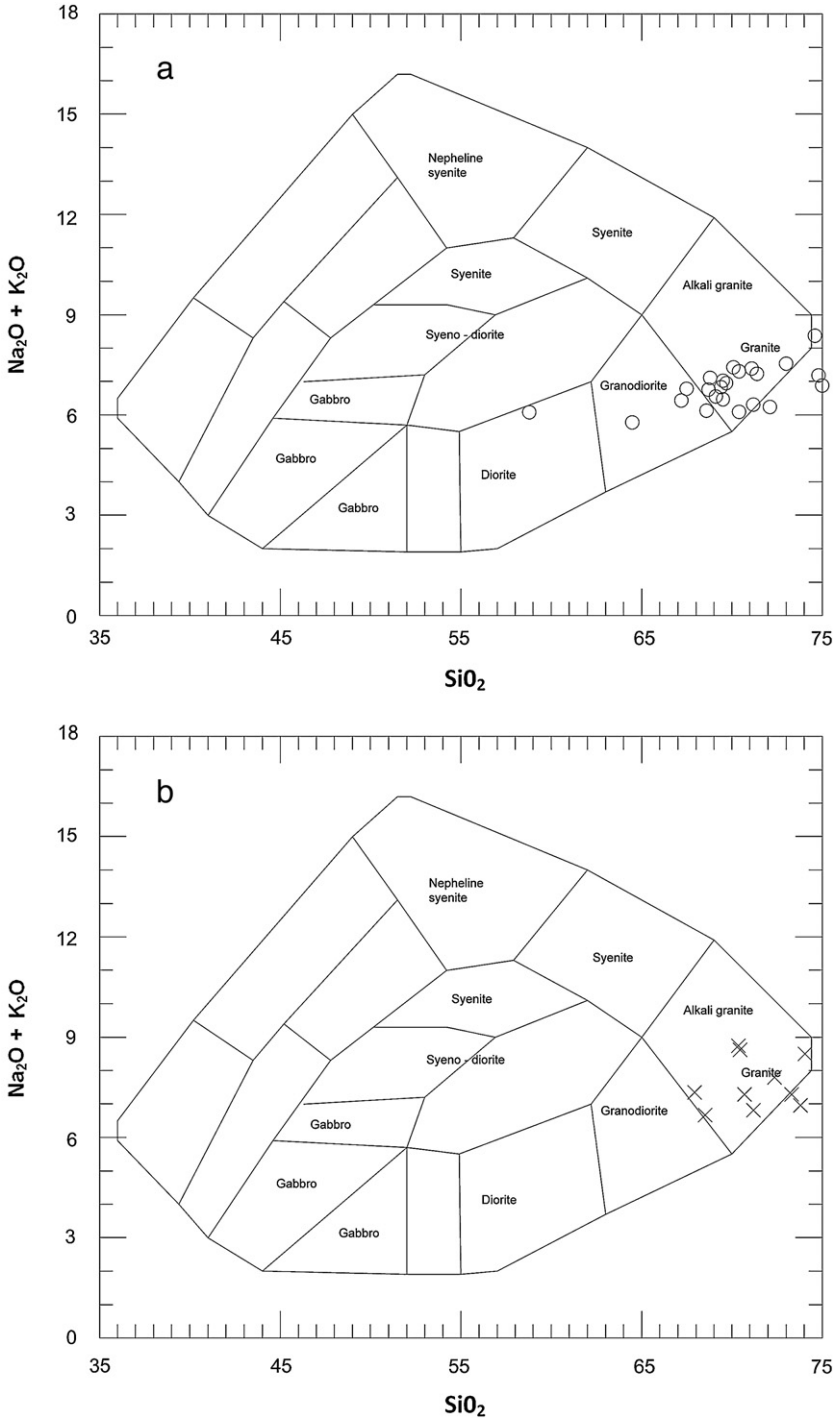

Fig. 2. (a). SiO_2 vs Total Alkalis diagram for I-type (open circles: ○) and (b) for S-type granites (crosses: ×).

the host granodiorite and do not provide a further indication for the isotopic composition of their mafic protolith.

6.2. Melting temperature in S-type granites

Based on results from melting experiments in peraluminous anatectic granites, it has been shown that for a given source composition and pressure, high temperature melts (high melt fraction in the protolith) have lower Al_2O_3/TiO_2 ratios than cooler melts where the degree of partial melting was lower (Sylvester, 1998, René et al., 2008).

Moreover, assuming that the differences in MgO and FeO between the S-type granites (leucogranites and biotite–granite) are not the result of fractionation processes alone, the concentrations of FeO and MgO contents can be used to roughly estimate melting temperatures (generating higher FeO and MgO contents with increasing temperature) (Scaillet et al., 1995; René et al., 2008). The higher MgO (and Fe_2O_{3tot}) (Fig. 5) the low Al_2O_3/TiO_2 (Fig. 6) as well as higher Zr and LREE (La + Ce) (Fig. 7) in the biotite-rich granites relative to the more leucocratic two-mica granites of Paros peraluminous S-type granites (Fig. 6) and compared to experimental results on melting metapelites, are compatible with higher temperature melts generated by dehydration melting reaction involving biotite. On the other hand the biotite-poor two-mica leucogranites are compatible with melt compositions generated by muscovite dehydration reactions.

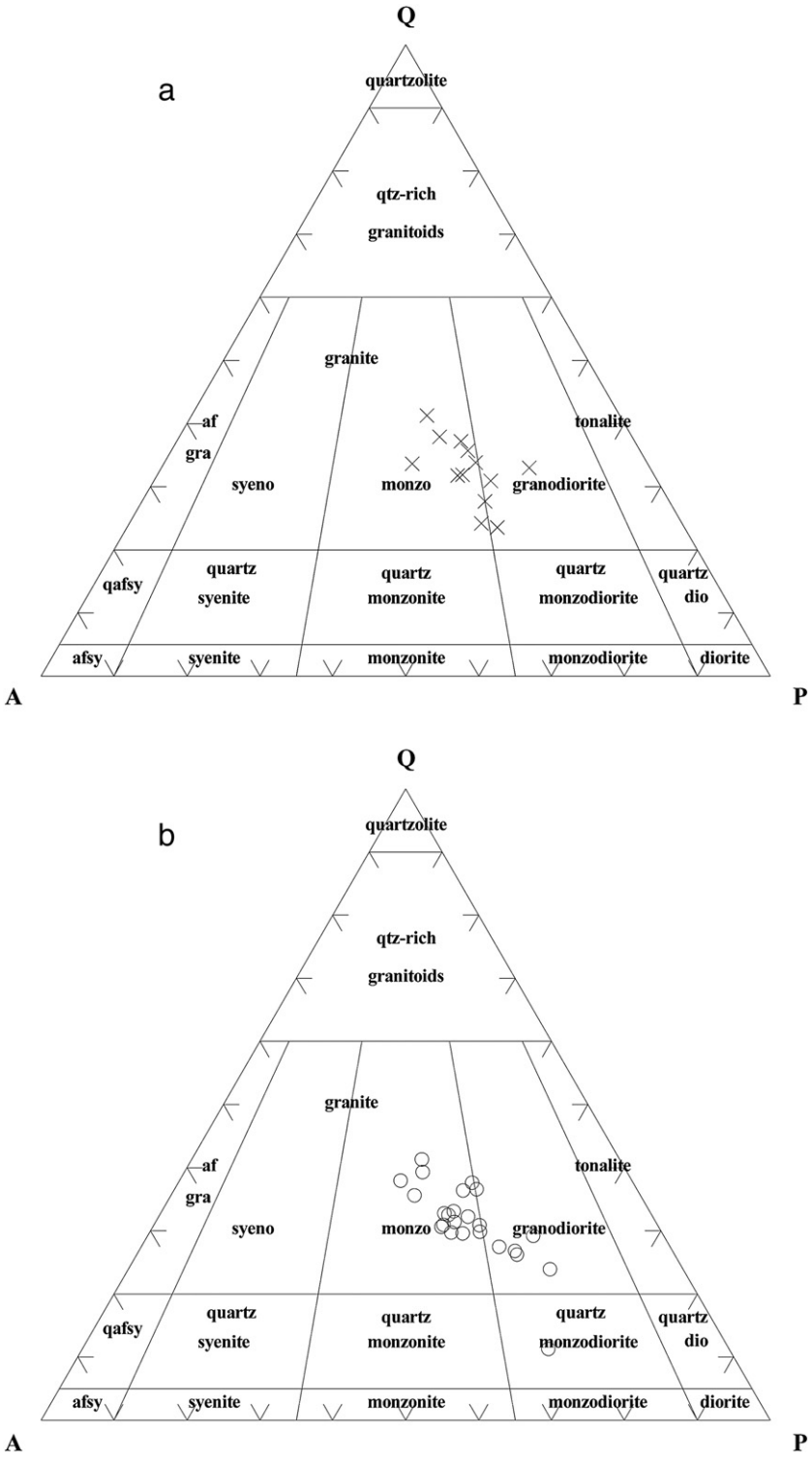

Fig. 3. (a) QAP classification diagram for I-type (open circles: ○) and (b) for S-type granites (crosses: ×).

Results from melting experiments have shown that dehydration melting reaction of muscovite in metapelites starts at ca. 700 °C and pressure ca. 5 kb (Thompson and Tracy, 1979), whereas biotite dehydration-melting may start at about 750 °C (Mogk, 1992).

6.3. Petrogenesis of the granitoids

Sr–Nd isotopic data of the upper Miocene granites from this study as well as Sr–Nd–Pb and O isotope data from previous studies (Altherr et al., 1988; Altherr and Siebel, 2002) are compatible with a metasedimentary crustal source for the generation of the Cyclades I- and S-type granitoids and do not necessarily require a mantle-derived component. The variation in ε_{Nd} values of both groups of granites lies within the range of the metasedimentary gneisses (Fig. 10), indicating that the Cyclades granites have a common metasedimentary crustal source similar to the exposed biotite gneiss country rocks (meta-greywacke). Previous isotope data on Cyclades granitoids documented a poor correlation between Nd–Sr isotopes within each pluton

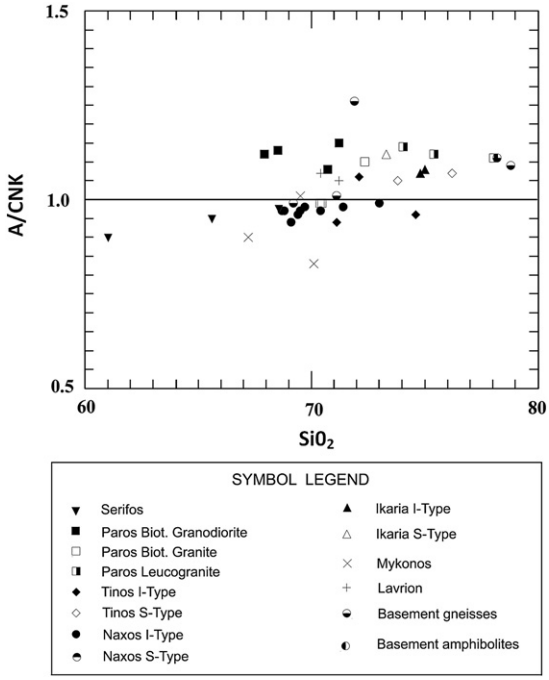

Fig. 4. SiO_2 vs A/CNK (Alumina saturation index, molar $Al_2O_3/(CaO/Na_2O+K_2O)$) for the Cyclades granitoids and basement gneiss samples.

(Altherr and Siebel, 2002) as well as between Nd–Sr and Pb isotope systems with major and trace elements (Juteau et al., 1986). These features probably indicate decoupling of the different isotopic systems which has been attributed to heterogeneities in the crustal source (Juteau et al., 1986) or different processes controlling the different isotope systems.

In the initial Nd vs Sr isotope diagram (Fig. 11) both of these types show overlapping fields and define a hyperbola trend, indicating mixing between two different end-member compositions, one clearly represented by the metasedimentary gneiss (Fig. 10).

Trace element variations indicate that biotite-gneisses can reproduce most of the trace element features of both granite types, yet there is a remarkable Sr-enrichment, coupled with Ca input. Metavolcanic rocks containing low-Ca amphiboles and biotite can undergo substantial dehydration melting, especially in Barrovian Facies Series (kyanite–sillimanite zone) at the same time as widespread metapelite dehydration melting (Thompson, 2001). It has been shown that in the pressure range of 4–6 kb (15–20 km depth of lithostatic pressure gradient) substantial overlap occurs between dehydration reactions and H_2O-saturated solidi. Thompson (2001), based on the above constraints, underlined that dehydration-melting occurs very close in temperature to H_2O-saturated melting, and it is most likely that some local H_2O-recycling may occur between the different partially melted rock types. The elevated Sr values, coupled with the absence of Sr anomaly and the low Y abundance may be attributed to dehydration melting of an amphibolite component. Yet experimental partial melting of such a mafic composition produces melts with high Sr, positive Sr anomaly and pronounced Y depletion. If mixing takes place in the source prior to the melting event, then silicic (granitic) melts would be followed by mafic (tonalite–diorite) partial melts as *P–T* increased, from the same crustal source, generating mixtures of these two end-members.

Melting experiment results on metagreywacke assemblages of biotite + plagioclase + quartz at 10–20 kb and 800 to 900 °C under fluid-absent conditions and with small amounts (2–4%) of water added, showed that biotite melting reaction occurs below 800 °C (at 10 kb) if 4% of water is added to the system, producing garnet + amphibole + melt (Gardien et al., 2000). The composition of such partial melts are Al_2O_3–SiO_2 rich and CaO–MgO poor and coexist with garnet and amphibole (10–15 kb), whereas the orthoclase content of the granitic melt varies from orthoclase-rich (10 kb) to orthoclase-poor (15–20 kb). It was also pointed out that growth of hornblende together with peraluminous granitic liquids requires addition of at least 2–4% H_2O. Gautier and Brun (1994) postulated that a possible source for the additional H_2O is the subsolidus breakdown of hydrous phases in adjacent pelitic and mafic compositions.

Phosphorous concentration in peraluminus anatectic granite liquids is buffered by apatite stability (Ayres and Harris, 1997). Experimental

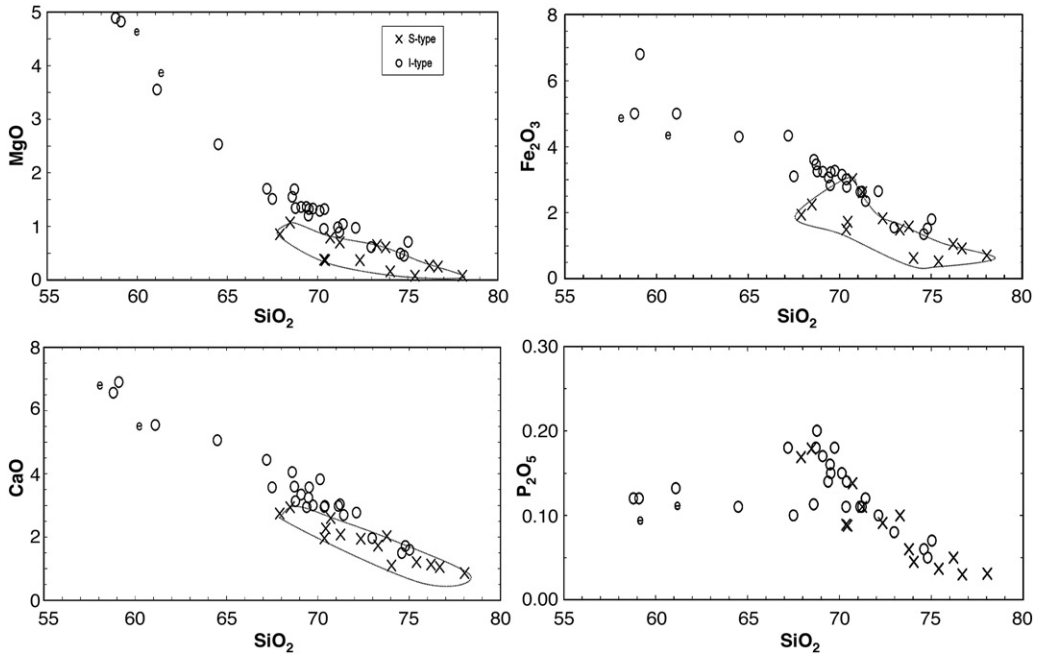

Fig. 5. Plots of selected major elements against silica for Cyclades granitoids and mafic enclaves (e) from the Serifos I-type pluton: MgO, CaO, $Fe2O_3$, P_2O_5. The outlined field correspond to the compositional field of the S-type granites, shown for better distinction (I-type: open circles ○, S-type: crosses: ×, enclaves of Serifos pluton: e).

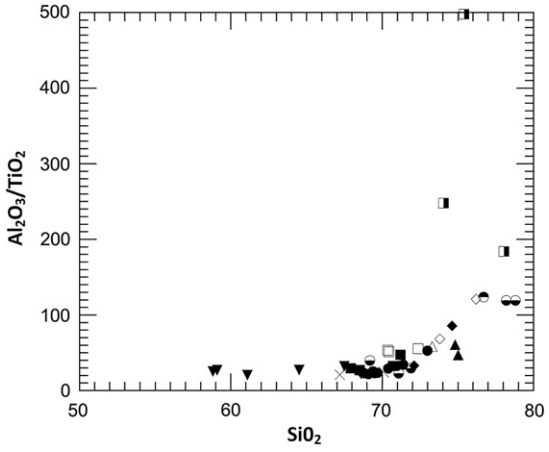

Fig. 6. Plot of the Al_2O_3/TiO_2 ratio vs SiO_2. Note that different groups of the S-type show distinctly different ranges of Al_2O_3/TiO_2. (e: enclaves, see legend Fig. 4).

results have shown that phosphorous saturation levels are a function of melt temperature and composition (Harrison and Watson, 1984; Wolf and London, 1994, 1995). It is suggested that the observed correlation of P_2O_5 with SiO_2 forming a common trend in both types of granites (I and S) can be attributed to mixing relationships as well as apatite fractionation (Fig. 5). The increase in P abundance in the S-type granites, starting from leucogranites to biotite granites to biotite granodiorites, may be explained with an increase in temperature of the melt (increasing degree of partial melting) with apatite being increasingly dissolved in the melt. Since apatite contains significant LREE concentrations, the broad correlation of P with La and Ce in the S-type granite series in Paros may also be explained as the effect of apatite during anatexis of the metasedimentary protolith with increasing temperature (Ayres and Harris, 1997) (Fig. 6).

Chemical differentiation within each pluton due to fractional crystallisation is not indicated by the variation trends in Harker diagrams, with the exception of the most evolved in SiO_2 granites, leucogranites and pegmatites/aplites (Fig. 7, Naxos I-, Paros Leucogranite and Ikaria).

6.4. Contribution of the marble component

One explanation for the shift in initial Sr isotope ratio towards a more depleted source observed in the S-type granitoids relative to the metasedimentary gneisses could be a mechanism of fluid interaction with intercalated marble layers within the gneiss unit. The isotopic Sr–Nd composition of marble from Santorini (Briqueu et al., 1986) of initial $^{87}Sr/^{86}Sr$: 0.708084 and initial $^{413}Nd/^{144}Nd$: 0.512594 is compatible with this hypothesis (Fig. 10). Such interactions are thought to be responsible for the equilibration of C and O isotope ratios of the high grade schists and interlayered marble bands during peak M2 conditions, in the Naxos migmatite dome (Baker et al., 1989; Baker and Matthews, 1994; Ganor et al., 1994). The observed increase in Sr and the Sr–O isotope downward shift have been similarly suggested to indicate source mixing of metapelites with carbonate sediments or Sr-rich marine formation waters (Bickle et al., 1988; Baker et al., 1989; Baker and Matthews, 1994).

Chemical and Sr–Nd isotopic variation can possibly be interpreted by a two-end-member mixing of: (1) a partial melt of the biotite-gneisses equivalent to greywacke-type metasediment, and (2) a Sr-rich metamorphic fluid, isotopically equilibrated with the marble horizons (Fig. 10). A hypothesis involving a mafic component derived

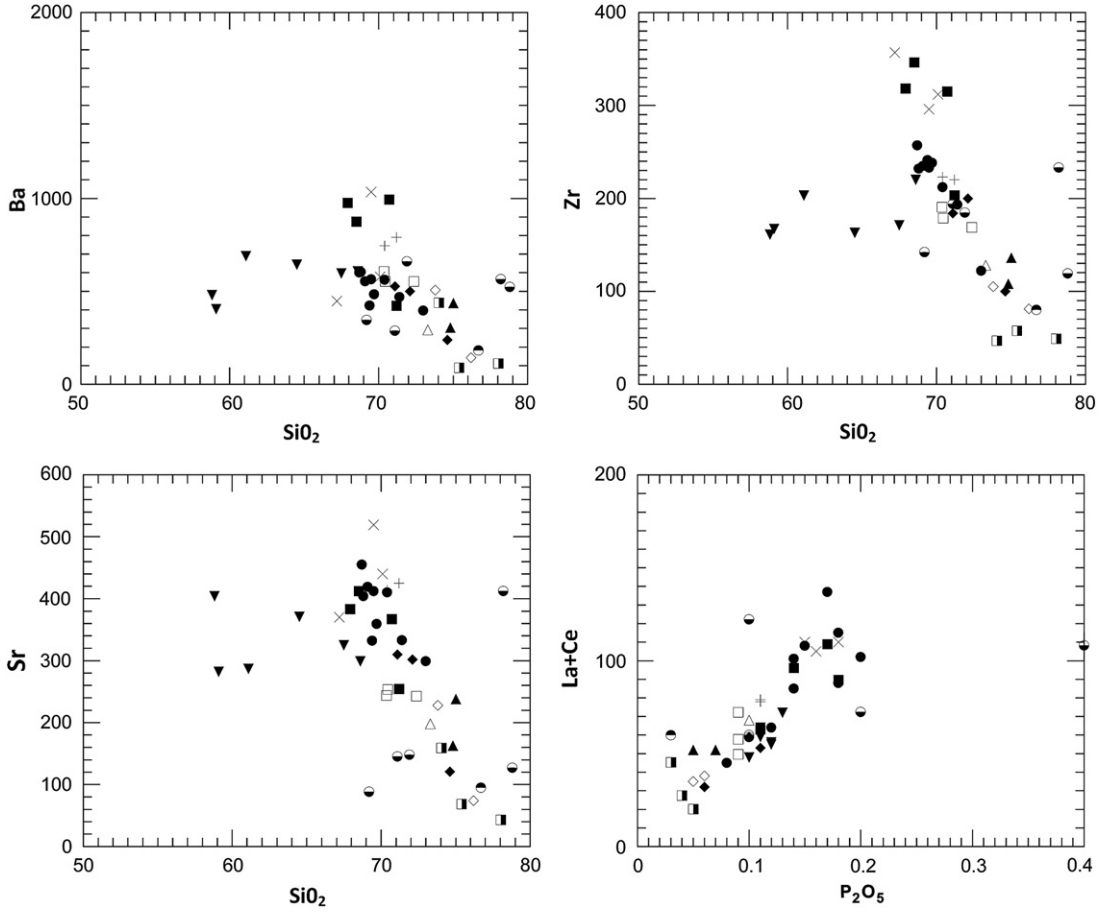

Fig. 7. Plots of selected trace elements against silica: a) Sr, b) Ba, c) Zr and (d) plot of P_2O_5 against La + Ce, for all Cyclades granitoids and basement gneisses (e: enclaves).

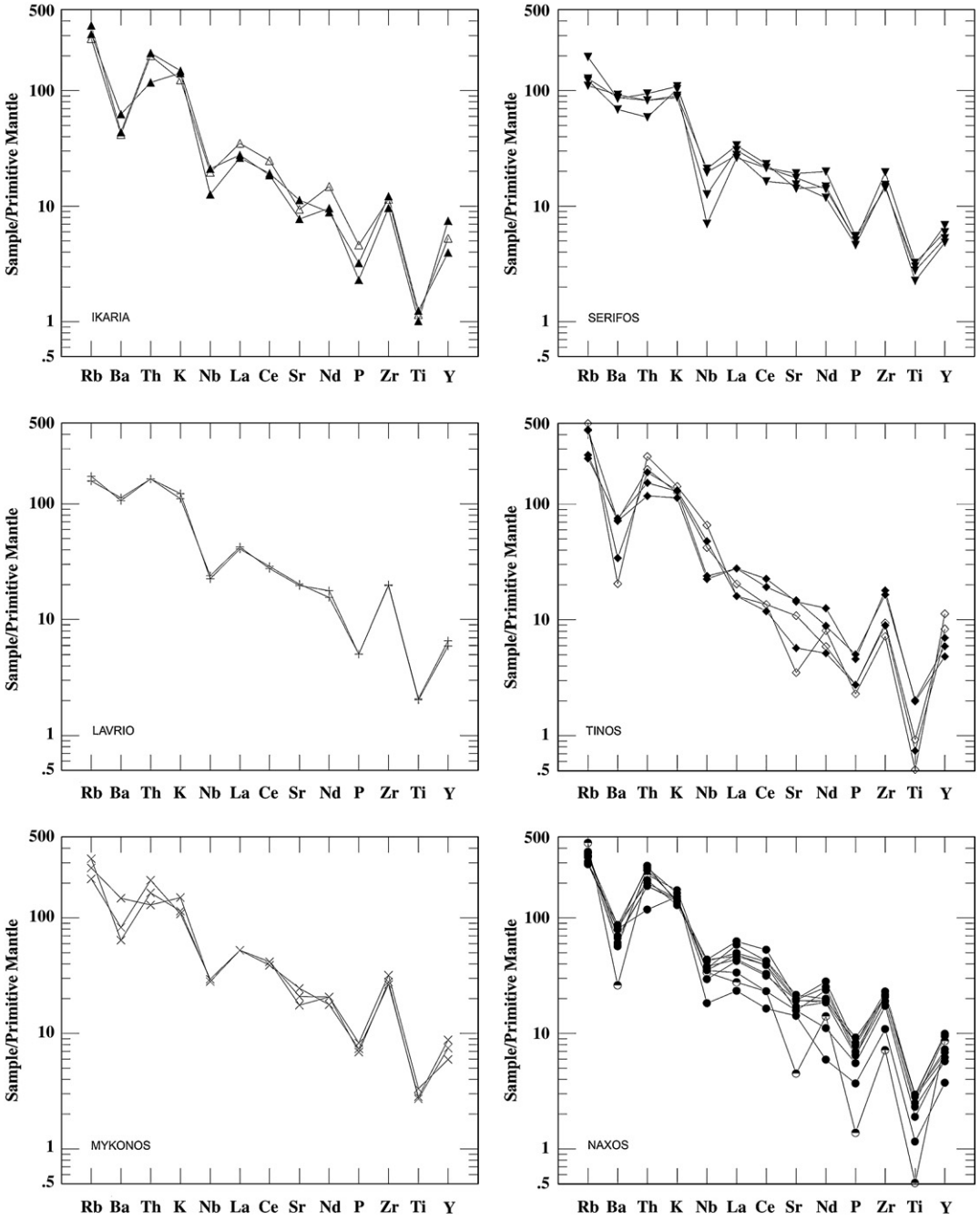

Fig. 8. Primordial mantle-normalised multi-element diagrams. (a) Cyclades I-Type granitoids (normalization values by McDonough et al., 1992).

from dehydration melting of an amphibolite rock cannot be excluded due to linear mixing relationships observed in the major element variations, the absence of a Sr anomaly, and the low Y abundance, in some of the I-type granitoids (e.g., Serifos and Lavrion).

6.5. Implications for the tectonic regime

Numerous radiometric, structural and seismic studies have shown that the Cyclades Miocene plutonism was contemporaneous with large scale crustal extension in the broad Aegean — Western Turkey region (Wijbrans and McDougall, 1988; Buick, 1991; Lee and Lister, 1992; Gautier and Brun, 1994; Brichau et al., 2008). The plutonism is closely associated with metamorphic core complexes (Naxos, Paros, Serifos and Mykonos), and some authors argue that the formation of core complexes in the Cyclades may have been triggered by heat input from intruded plutons, sills and dykes beneath the gneiss domes during short-lived thermal pulses (Lister and Baldwin, 1993). Subsequent isostatic rebound or inflation of sills caused differential uplift of the core complexes. The ductile to brittle transition observed in the gneiss domes of Naxos, Paros and Los and the mylonitic fronts on Mykonos, Ikaria and Tinos plutons is considered to be evidence of cooling beneath ductile shear zones after the intrusive event.

7. Conclusions

The following conclusions can be drawn from these data concerning the petrogenesis of the Cyclades granites:

1. Sr, Nd (and O) isotopic ratios of Cyclades granites confirm that they are derived from a crustal source. The source rocks are heterogeneous in terms of Sr isotopes but rather confined in terms of Nd

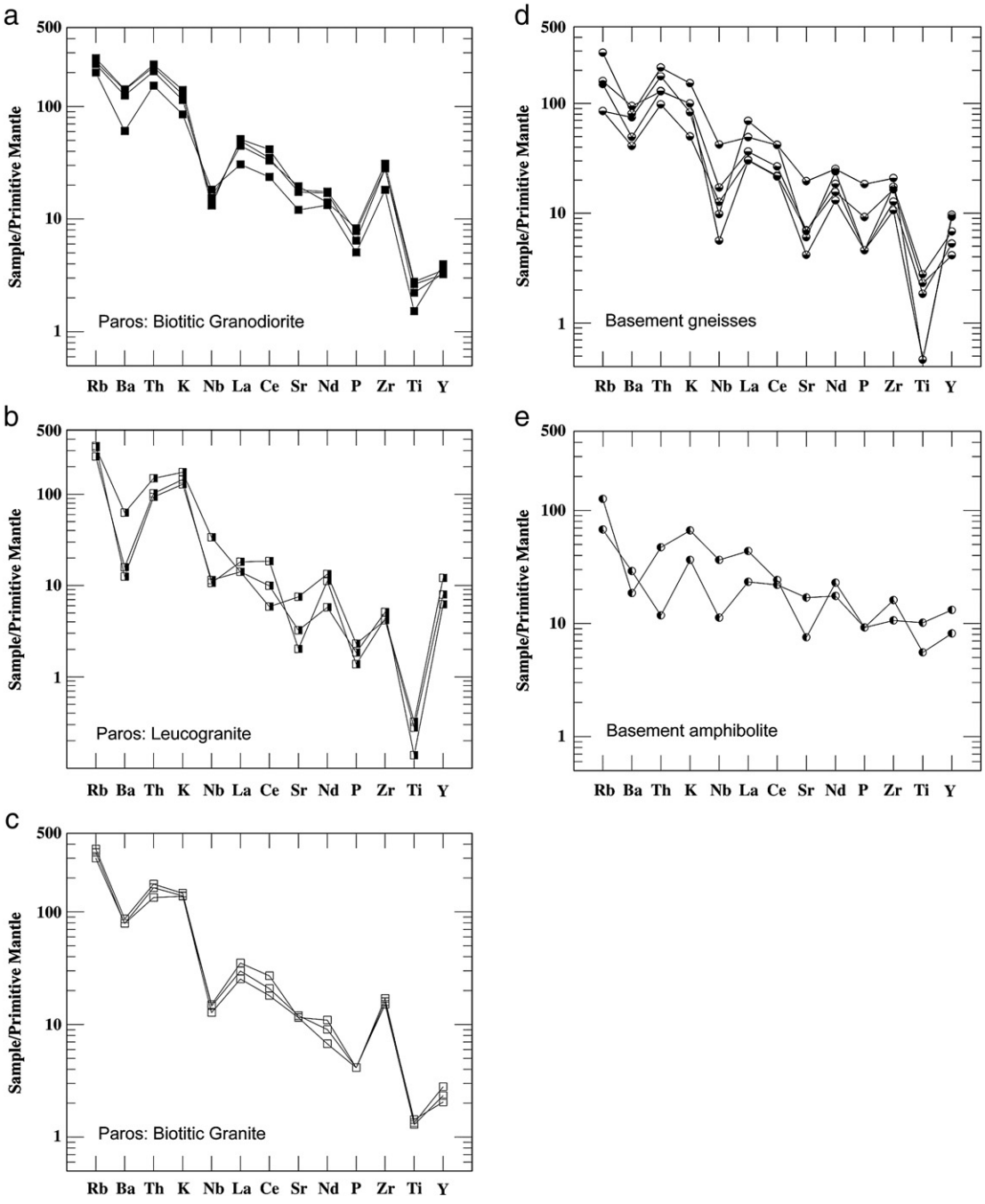

Fig. 9. Primordial mantle-normalised multielement diagrams for representative S-type granitoids of Paros: (a) biotite–granodiorite, (b) leucogranite, (c) biotite–granite, (d) basement gneiss and (e) amphibolites.

isotopes, and are probably largely sedimentary in origin. Compared with the isotopic Sr–Nd–O isotopic composition of the contemporaneous extrusive and intrusive rocks in the eastern Aegean, it would appear that a contribution from a high-K isotopically enriched mantle-derived magma source is not required.

2. The most mafic granites from the Paros metamorphic complex display transitional S/I-type characteristics, both in terms of major and trace elements and in their Sr isotope composition which extends beyond the range of the metasedimentary gneisses. The observed shift of initial Sr isotope ratio of these granites as well as for all the I-type granitoids towards a more depleted source is best explained if the I-type and the S/I granitoids are derived from a similar but deeper crustal source. This conclusion is consistent with earlier suggestions that the voluminous I-type intrusions were possibly generated by dehydration melting of metaluminous older crustal sources, e.g. of metagreywacke type (Altherr and Siebel, 2002).
3. Variations in major elements with partial overlap between I- and S-type granites and characteristic clustering in trace element variation support the hypothesis that mixing between mafic and acidic end-members operated in the source (at depth) and the bulk composition of each pluton reflects a certain degree of chemical and isotopic homogenisation between different components. Hybridization between a tonalite magma (I-type melts) similar to the composition of Serifos enclaves and granitic (silicic S-type melts) is demonstrated by from the existence of mafic microgranular enclaves in most I-type

Table 3
Rb–Sr and Sm–Nd isotope data from Cycladic granites, Naxos migmatite, basement gneiss and metabasic rocks (amphibolites).

Sample	Type	Rb	Sr	Rb/Sr	$^{87}Rb/^{86}Sr$	$^{87}Sr/^{86}Sr_{(m)}$	$(^{87}Sr/^{86}Sr)i$	Sm	Nd	$^{147}Sm/^{144}Nd$	$^{143}Nd/^{144}Nd_{(m)}$	$(^{143}Nd/^{144}Nd)_i$	ε_{Nd}
Granites													
LA-3	I-type	100	425	0.24	0.681	0.710195	0.71010	5.31	28.3	0.113	0.512161	0.51215	−9.2
SER-1	I-type	81	299	0.27	0.787	0.711339	0.71124	5.47	27.6	0.120	0.512191	0.51218	−8.6
SER-26	I-type	124	325	0.38	1.105	0.710288	0.71015	4.42	26.7	0.119	0.512305	0.51230	−6.4
SER-56	I-type	70	371	0.19	0.543	0.719158	0.70909	4.25	20.9	0.123	0.512313	0.51231	−6.3
SER-30	I-type	78	405	0.19	0.559	0.710349	0.71028	5.89	26.7	0.134	0.512233	0.51223	−7.8
IK-1	I-type	196	238	0.82	2.384	0.713038	0.71277	4.98	23.7	0.127	0.512205	0.51219	−8.3
IK-2	S-type	179	198	0.90	2.618	0.71643	0.71587	3.80	19.2	0.120	0.512114	0.51210	−10.1
MYK-1	I-type	172	519	0.33	0.959	0.711535	0.71138	8.14	42.5	0.116	0.512155	0.51215	−9.3
MYK-3	I-type	206	440	0.31	0.908	0.711611	0.71147	7.69	41.2	0.113	0.512098	0.51209	−10.4
NAX-1 N	I-type	235	333	0.71	2.043	0.711246	0.71088	4.62	25.2	0.111	–	–	–
NAX-5	I-type	189	455	0.42	1.202	0.710989	0.71077	7.65	44.1	0.105	0.512188	0.51219	−8.6
NAX-10	I-type	213	410	0.52	1.504	0.711252	0.71098	6.17	34.8	0.107	0.512210	0.51221	−8.2
TI-3	I-type	158	310	0.51	1.475	0.711763	0.71138	4.09	20.3	0.122	0.512223	0.51221	−7.9
TI-4	I-type	169	302	0.56	1.615	0.711769	0.71151	4.03	21.7	0.112	0.512239	0.51223	−7.6
TI-6	S-type	276	228	1.21	3.503	0.710729	0.71003	3.63	15.7	0.140	0.512236	0.51222	-7.5
PA—4	S- (Leucogr.)	213.8	68.3	3.14	9.11	0.713966	0.711637	2.68	9.38	0.1727	0.512186	0.512166	−8.8
PA-15	S- (Leucogr.)	164.1	42.7	3.81	11.1	0.765263	0.762426	5.52	18.1	0.1844	0.512236	0.512214	−7.8
PA-9	S- (Tr- Gt- Pgm.)	206.7	158.9	1.3	3.77	0.714229	0.713265	2.38	7.23	0.1994	0.512173	0.51215	−9.1
PR-4	S- (Bit Gr.)	151	245.8	0.94	2.92	0.712228	0.711482	4.5	24	0.1134	0.5122	0.512187	−8.4
P-5	S- (Bit Gr.)	229.1	243.5	0.94	2.72	0.712215	0.711519	4.86	26.25	0.112	0.512208	0.512195	−8.2
PA-13	S- (Bit Grd)	158.6	383	0.41	1.2	0.712002	0.711695	5.99	37.84	0.0956	0.512191	0.51218	−8.5
P-14	S- (Bit Gr.)	189.9	253.3	0.75	2.17	0.712395	0.71184	3.4	18.86	0.1088	0.512181	0.512168	−8.7
Basement rocks													
PR-6	Gneiss	101.4	150.7	0.68	2.02	0.717837	0.717321	2.99	37.68	0.048	0.512128	0.512122	−9.6
SR93-52	Gneiss	60.1	144	0.418	1.21	0.716267	0.716112	7.04	35.5	0.1985	0.5122	0.512193	−8.4
SR93-20	Amphibolite	43	357	0.12	0.3525	0.705127	0.705082	6.42	62.85	0.1444	0.512856	0.512847	4.3
NX-13	Amphibolite in migmatite	80	159	0.50	1.456	0.710267	0.71000	8.35	32.9	0.153	0.512519	0.51252	−2.2
Average Paros gneiss ($n=9$)		136	150	0.91	2.73	0.71860	0.71790	6.00	36.8064	0.1123	0.512164	0.512151	−9.0

composite intrusions and the absence of clear contacts between the different petrological facies in the same composite pluton (Altherr et al., 1988).

4. Trace element variations among the various S-type granites and the metasedimentary sources indicate that a metasedimentary component, similar to an immature greywacke type which is the most common type of sediment within the gneissic basement of Cyclades, can reproduce most of the trace element patterns in the normalised multi-element diagrams. Decompression melting of the crust must have taken place at increasing temperature, where dehydration melting of muscovite was followed by biotite dehydration melting reaction at possibly mid-crustal levels where garnet was not stable.
5. Some regional variations are observed in terms of trace elements: the central Cyclades plutons (Naxos and Mykonos) display a greater enrichment in LILE and LREE, possibly as temperature of melting increased under rapid decompressional conditions. It is suggested that amphibolite is another end-member which contributes mostly to the source of the younger intrusions, at the western flank of the arc, as decompression melting in the Cyclades crust preceeded with time at progressively deeper structural levels (e.g., Serifos and Lavrion).

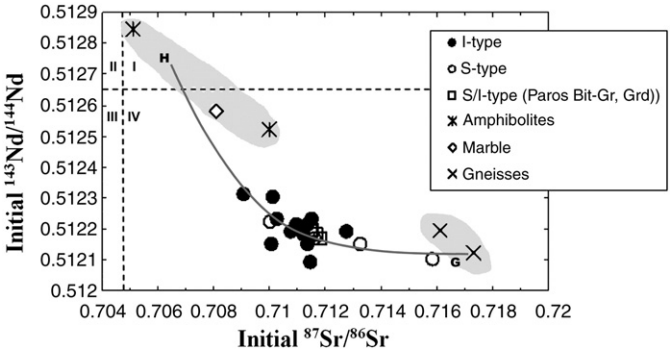

Fig. 10. Initial $^{87}Sr/^{86}Sr$ vs Initial $^{143}Nd/^{144}Nd$ ratios for Cyclades granitoids (see Table 1) and various basement rocks (gneiss, amphibolite and marble). Hyperbolic mixing curve (H–G) defined by $^{87}Sr/^{86}Sr$ and $^{143}Nd/^{144}Nd$ ratios of a metasedimentary greywacke-type Gneiss (G), and a mafic component with hypothetical composition (H), represented by a mixed amphibolite + marble component. Note that granite and gneiss samples confine the isotopic composition of the metasedimentary end-member (G). (End-member compositions, G: Sr = 150 ppm, Nd = 37 ppm, initial $^{87}Sr/^{86}Sr = 07173$, initial $^{143}Nd/^{144}Nd = 051212$ — H: Sr = 350 ppm, Nd = 18, Initial $^{87}Sr/^{86}Sr = 0.7064$, Initial $^{143}Nd/^{144}Nd = 0.51275$, Santorini marble by Briqueu et al., 1986).

Acknowledgements

We acknowledge the General Secretariat of Research and Technology (GGET) — Ministry of Development of Greece for financially supporting this work. Nick Marsh is thanked for performing the XRF analytical work. Charalabos Vasilatos is thanked for invaluable help with figures reconstruction. Finally, we would like to thank H. Downes for a very detailed and constructive review.

References

Altherr, R., Siebel, W., 2002. I-type plutonism in a continental back-arc setting: Miocene granitoids and monzonites from the central Aegean Sea, Greece. Contributions to Mineralogy and Petrology 143, 397–415.
Altherr, R., Kreuzer, H., Wendt, I., Lenz, H., Wagner, G.A., Keller, J., Harre, W., Hohndorf, A., 1982. A late Oligocene/early Miocene high temperature belt in the Attic–Cycladic crystalline complex (SE Pelagonian, Greece). Geologisches Jahrbuch E23, 97–164.
Altherr, R., Henjes-Kunst, F.J., Matthews, A., Friedrichsen, H., Hansen, B.T., 1988. O–Sr isotopic variations in Miocene granitoids from the Aegean: evidence for an origin by combined assimilation and fractional crystallisation. Contributions to Mineralogy and Petrology 100, 528–541.
Andriessen P.A.M., 1978. Isotopic age relations within the polymetamorphic complex of the island of Naxos (Cyclades, Greece) PhD thesis State University Utrecht.
Andriessen, P.A.M., Boelrijk, N.A.I.M., Hebeda, E.H., Priem, E.N.A., Verdurmen, E.A.Th., Verschure, R.H., 1979. Dating the events of metamorphism and granitic magmatism in the Alpine orogen of Naxos (Cyclades, Greece). Contributions to Mineralogy and Petrology 69, 215–225.

Andriessen, P.A.M., Banga, G., Hebeda, E.H., 1987. Isotopic age study of pre-Alpine rocks in the basal units on Naxos, Sikinos and Ios, Greek Cyclades. Geologie en Mijnbouw 66, 3–14.
Avigad, D., Garfunkel, Z., 1991. Uplift and exhumation of high-pressure metamorphic rocks: the example of the Cycladic blueschist belt (Aegean Sea). Tectonophysics 188, 357–372.
Avigad, D., Baer, G., Heimann, A., 1998. Block rotation and continental extension in the central Aegean Sea: paleomagnetic and structural evidence from Tinos and Mykonos (Cyclades, Greece). Earth and Planetary Science Letters 157, 23–40.
Ayres, M., Harris, N., 1997. REE fractionation and Nd-isotope disequilibrium during crustal anatexis: constraints from Himalayan leucogranites. Chemical Geology 139, 249–269.
Baker, J., Matthews, A., 1994. Textural and isotopic development of marble assemblages during the Barrovian-style M2 metamorphic event, Naxos, Greece. Contributions to Mineralogy and Petrology 116, 130–144.
Baker, J., Bickle, M.J., Buick, I.S., Holland, T.J.B., Matthews, A., 1989. Isotopic and petrological evidence for the infiltration of water-rich fluids during the Miocene M2 metamorphism on Naxos, Greece. Geochimica et Cosmochimica Acta 53, 2037–2050.
Baldwin, S.L., Lister, G.S., 1994. P–T–t paths of Aegean metamorphic core complexes: Ios, Paros and Syros. US Geological Survey Circular 19.
Baldwin, S.L., Lister, G.S., 1998. Thermochronology of the South Cyclades Shear Zone, Ios, Greece: effects of ductile shear in the argon partial retention zone. Journal of Geophysical Research 103, 7315–7336.
Baltatzis, E., 1996. Blueschist-to-greenschist transition and the P–T path of the prasinites from the Lavrion area, Greece. Mineralogical Magazine 60, 551–561.
Bickle, M.J., Wickham, S.M., Chapman, H.J., Taylor, H.P., 1988. A strontium, neodymium and oxygen isotope study of hydrothermal metamorphism and crustal anatexis in the Trois Seigneurs Massif, Pyrenees, France. Contributions to Mineralogy and Petrology 100, 399–417.
Brichau, S. 2004. Constraining the tectonic evolution of extensional fault systems in the Cyclades Greece using low-temperature thermochronology. PhD thesis, University of Mainz, Germany.
Brichau, S., Thomson, S., Ring, U., 2008. Thermochronometric constraints on the tectonic evolution of the Serifos detachment, Aegean Sea, Greece. International Journal of Earth Sciences 1437–3254. doi:10.1007/s00531-008-0386-0.
Briqueu, L., Javoy, M., Lancelot, J.R., Tatsumoto, M., 1986. Isotope geochemistry of recent magmatism in the Aegean arc: Sr, Nd, Hf, and O isotopic ratios in the lavas of Milos and Santorini — geodynamic implications. Earth and Planetary Science Letters 80, 41–54.
Bröcker, M., Franz, L., 1998. Rb–Sr isotope studies on Tinos island (Cyclades, Greece): additional time constraints for metamorphism, extent of infiltration-controlled overprinting and deformational activity. Geological Magazine 135, 369–382.
Bröcker, M., Kreuzer, H., Matthew, A., Okrusch, M., 1993. $^{40}Ar/^{39}Ar$ and oxygen isotope studies of polymetamorphism from Tinos island, Cycladic blueschist belt, Greece. Journal of Metamorphic Geology 11, 223–240.
Brown, M., 1994. The generation, segregation, ascent and emplacement of granite magma: the migmatite-to-crustally-derived granite connection in thickened orogens. Earth Science Reviews 36, 83–130.
Buick, I.S., 1988. The metamorphism and structural evolution of the Barrovian overprint, Naxos, Greece. PhD thesis, University of Cambridge.
Buick, I.S., 1991. The late Alpine evolution of an extensional shear zone, Naxos, Greece. Journal of the Geological Society of London 148, 93–103.
Buick, I.S., Holland, T.J.B., 1989. The P–T–t path associated with crustal extension, Naxos, Cyclades, Greece. In: Daly, J.S., Cliff, R.A., Yardley, B.W.D. (Eds.), Evolution of Metamorphic Belts: Geological Society of London Special Publication, vol. 43, pp. 365–370.
Chappell, B.W., White, A.J.R., 1974. Two contrasting granite types. Pacific Geology 8, 173–174.
Chappell, B.W., White, A.J.R., 1992. I-type and S-type granites in the Lachlan Fold Belt. Transactions of the Royal Society of Edinburgh: Earth Sciences 83, 1–26.
Cox, K.G., Bell, J.D., Pankhurst, R.J., 1979. The interpretation of igneous rocks. George Allen & Unwin, London. 445 pp.
Duchêne, S., Aïssa, R., Vanderhaeghe, O., 2006. Pressure-temperature-time evolution of metamorphic rocks from Naxos (Cyclades, Greece): constraints from thermobarometry and Rb/Sr dating. Geodinamica Acta 19 (5), 301–321.
Dürr, S., Altherr, R., Keller, J., Okrush, M., Seider, E., 1978. The median Aegean crystalline belt: stratigraphy, structure, metamorphism, magmatism. In: Cloos, H., Roeder, D., Schmidt, K. (Eds.), Alps, Apennines, Hellenides. Schweiz Barts'che Verlag, Stuttgart, pp. 455–477.
Forster, M.A., Lister, G.S., 1999. Detachment faults in the Aegean Core Complex of Ios, Greece. In: Ring, U., Brandon, M.T., Lister, G.S., Willett, S.D. (Eds.), Exhumation Processes: Normal Faulting, Ductile Flow and Erosion: Geological Society, London, Special Publications, 154, pp. 305–323.
Ganor, J., Matthews, A., Schliestedt, M., 1994. Post metamorphic low δ13C calcite veins in the Cycladic complex (Greece) and their implications for modelling fluid infiltration processes using carbon isotope compositions. Eurioean. Journal of Mineralogy 6, 365–379.
Gardien, V., Thompson, A.B., Ulmer, P., 1999. Melting of biotite + plagioclase + quartz gneisses: the role of H_2O in the stability of amphibole. Journal of Petrology 41, 651–666.
Gardien, V., Thompson, A.B., Ulmer, P., 2000. Melting of Biotite + Plagioclase + Quartz Gneisses: the Role of H_2O in the Stability of Amphibole. Journal of Petrology 41 (5), 651–666.
Gautier, P., Brun, J.-P., 1994. Crustal-scale geometry and kinematics of late-orogenic extension in the central Aegean (Cyclades and Evvia Island). Tectonophysics 238, 399–424.
Henjes-Kunst, F., Altherr, R., Kreuzer, H., Hansen, B.T., 1988. Disturbed U–Th–Pb systematics of young zircons and uranothorites: the case of the Miocene Aegean granitoids (Greece). Chemical Geology 73, 125–145.
Harrison, T.M., Watson, E.B., 1984. The behaviour of apatite during crustal anatexis: Equilibrium and kinetic considerations. Geochimica et Cosmochimica Acta 48, 1467–1477.
Iglseder, C., Grasemann, B., Schneider, D.A., Petrakakis, K., Miller, C., Klötzli, U.S., Thöni, M., Zámolyi, A., Rambousek, C., 2008. I and S-type plutonism on Serifos (W-Cyclades, Greece). Tectonophysics. doi:10.1016/j. tecto.2008.09.021.
Jansen, J.B.H., Schuiling, R.D., 1976. Metamorphism on Naxos: petrology and geothermal gradients. American Journal of Science 276, 1225–1253.
Johnston, A.D., Wyllie, P.J., 1988. Constraints on the origin of Archean trondhjemites based on phase relationships of Nük gneiss with H_2O at 15 kbar. Contributions to Mineralogy and Petrology 100, 35–46.
Juteau, M., Michard, A., Albarède, F., 1986. The Pb–Sr–Nd isotope geochemistry of some recent circum-Mediterranean granites. Contributions to Mineralogy and Petrology 92, 331–340.
Keay, S., 1998. The geological evolution of the Cyclades, Greece: constraints from SHRIMP U–Pb geochronology (Ph.D. thesis): Canberra, Australian National University.
Keay, S., Lister, G., 2002. African provenance for the metasediments and metaigneous rocks of the Cyclades, Aegean Sea, Greece. Geology 30, 235–238.
Keay, S., Lister, G., Buick, I., 2001. The timing of partial melting, Barrovian metamorphism and granite intrusion in the Naxos metamorphic core complex, Cyclades, Aegean Sea, Greece. Tectonophysics 342, 275–312.
Lee, J., Lister, G.S., 1992. Late Miocene ductile extension and detachment faulting, Mykonos, Greece. Geology 20, 121–124.
Lesher, C.E., 1990. Decoupling of chemical and isotopic exchange during magma mixing. Nature 344, 235–237.
Lister, G.S., Baldwin, S.L., 1993. Plutonism and the origin of metamorphic core complexes. Geology 21, 607–610.
Lister, G.S., Banga, G., Feenstra, A., 1984. Metamorphic core complex of Cordilleran type in the Cyclades, Aegean Sea, Greece. Geology 12, 221–225.
Marsh, N.G., Tarney, J., Hendry, G.L., 1983. Trace element geochemistry of basalts from hole 504B, Panama Basin, DSDP Legs 69 & 70. Init Rep DSDP 69, 747–764.
McDonough, W.F., Sun, S., Ringwood, A.E., Jagoutz, E., Hofmann, A.W., 1992. K, Rb and Cs in the earth and moon and the evolution of the earth's mantle. Geochimica et Cosmochima Acta 56, 1001–1012.
McGrath, A., 1999. Structural and geochemical evolution of an extensional metamorphic core complex, Paros, Greece. PhD thesis, University of Leicester,UK.
Mogk, D.W., 1992. Ductile shearing and migmatization at mid crustal levels in an Archean high grade gneiss belt, northern Gallatin Range, Montana, USA. Journal of Metamorphic Geology 10, 427–438.
Patiño-Douce, A.E., Beard, J.S., 1995. Dehydration-melting of biotite gneiss and quartz amphibolite from 3 to 15 kb. Journal of Petrology 36, 707–738.
Pe-Piper, G., 2000. Origin of S-type granites coeval with I-type granites in the Hellenic subduction system, Miocene of Naxos, Greece. European Journal of Mineralogy 12, 859–875.
Pe-Piper, G., Kotopouli, C.N., Piper, D.J.W., 1997. Granitoid rocks of Naxos, Greece: regional geology and petrology. Geological Journal 32, 153–171.
Pe-Piper, G., Piper, D.J.W., Matarangas, D., 2002. Regional implications of geochemistry and style of emplacement of Miocene I-type diorite and granite, Delos, Cyclades, Greece. Lithos 60, 47–66.
Reischmann, T., 1998. Pre-Alpine origin of tectonic units from the metamorphic complex of Naxos, Greece, identified by single zircon Pb/Pb dating. Bulletin of Geological Society of Greece XXXII/3, 101–111.
René, M., Holtz, F., Luo, C., Beermann, O., Stelling, J., 2008. Biotite stability in peraluminous granitic melts: compositional dependence and application to the generation of two-mica granites in the South Bohemian batholith (Bohemian Massif, Czech Republic). Lithos 102, 538–553.
Ring, U., Gessner, K., Güngör, T., Passchier, C.W., 1999. The Menderes Massif of western Turkey and the Cycladic Massif in the Aegean- do they really correlate? Journal of the Geological Society 156, 3–6.
Rushmer, T., 1991. Partial melting of two amphibolites: contrasting results under fluid-absent conditions. Contributions to Mineralogy and Petrology 107, 41–59.
Scaillet, B., Pichavant, M., Roux, J., 1995. Experimental crystallization of leucogranite magmas. Journal of Petrology 36, 663–705.
Salemink, J., 1980. On the geology and petrology of Serifos Island (Cyclades, Greece). Annual Geology Pays Hellenic 30, 342–365.
Skarpelis, N., Tsikouras, B., Pe-Piper, G., 2008. The Miocene igneous rocks in the Basal Unit of Lavrion (SE Attica, Greece): petrology and geodynamic implications. Geological Magazine 145, 1–15.
Skjerlie, K.P., Johnston, A.D., 1996. Vapor absent melting from 10 to 20 kbar of crustal rocks that contain multiple hydrous phases: implications for anatexis in the deep to very deep continental crust and active continental margins. Journal of Petrology 37, 661–691.
Storkey, A.C., Hermann, J., Hand, M., Buick, I.S., 2005. Using in situ trace-element determinations to monitor partial-melting processes in metabasites. Journal of Petrology 46, 1283–1308.
Stouraiti C., 1995. Geochemistry and petrogenesis of the Serifos granite in relation to other Aegean granitoids, Greece. PhD thesis, University of Leicester, UK, 239 pp.
Sylvester, P.J., 1998. Post-collisional strongly peraluminous granites. Lithos 45, 29–44.
Thompson, A.B., 1982. Dehydration melting of crustal rocks and the generation of H_2O-undersaturated granitic liquids. American Journal of Science 282, 1567–1595.
Thompson, A.B., 1996. Fertility of crustal rocks during anatexis. Transactions of the Royal Society of Edinburgh: Earth Sciences 87, 1–10.
Thompson, A.B., 2001. Partial melting of metavolcanics in amphibolite facies regional metamorphism. Proceedings of the Indian Academy of Science (Earth and Planetary Science) 110 (No. 4), 287–291.

Thompson, A.B., Tracy, R.J., 1979. Model systems for anatexis of politic rocks: II. Facies series melting and reactions in the system CaO-KAlO2-NaAlO2-Al2O3-SiO2-H2O. Contributions to Mineralogy and Petrology 70, 429–438.

Thompson, A.B., Ellis, D.J., 1994. $CaO + MgO + Al_2O_3 + SiO_2 + H_2O$ to 35 kb: amphibolite, talc, and zoisite dehydration and melting reactions in the silica-excess part of the system and their possible significance in subduction zones, amphibolite melting, and magma fractionation. American Journal of Science 294, 1229–1289.

Van Der Maar, P.A., Jansen, J.B.H., 1983. The geology of the polymetamorphic complex of Ios, Cyclades, Greece and its significance for the Cycladic Massif. Geologische Rundschau 72, 283–299.

Vielzeuf, D., Holloway, J.R., 1988. Experimental determination of the fluid-absent melting reactions in the pelitic system. Contributions to Mineralogy and Petrology 98, 257–276.

Wedepohl, K.H., 1995. The composition of the continental crust. Geochimica et Cosmochimica Acta 59, 1217–1232.

White, R.W., Powell, R., Clarke, G.L., 2003. Prograde metamorphic assemblage evolution during partial melting of metasedimentary rocks at low pressures: migmatites from Mt Stafford, central Australia. Journal of Petrology. 44, 1937–1960.

Wijbrans, J.R., McDougall, I., 1988. Metamorphic evolution of the Attic Cycladic Massif Belt on Naxos (Cyclades, Greece) utilizing $^{40}Ar/^{39}Ar$ age spectrum measurements. Journal of Metamorphic Geology 6, 1–23.

Wolf, M.B., London, D., 1994. Apatite dissolution into peraluminoushaplogranitic melts: an experimental study of solubilities and mech-anisms. Geochimica et Cosmochimica Acta 58, 4127–4145.

Wolf, M.B., London, D., 1995. Incongruent dissolution of REE- and Sr-rich apatite in peraluminous granitic liquids: differential apatite, monazite, and xenotime solubilities during anatexis. American Mineralogist 80, 765–775.

Wolf, M.B., Wyllie, P.J., 1991. Dehydration-melting of solid amphibolite at 10 kb: textural development, liquid interconnectivity and applications to the segregation of magmas. Contributions to Mineralogy and Petrology 44, 151–179.

Wyllie, P.J., Wolf, M.B., 1993. Amphibolite dehydration melting: sorting out the solidus. In: Prichard, H.M., Alabaster, T., Harris, N.B.W., Neary, C.R. (Eds.), Magmatic Processes and Plate Tectonics: Geological Society of London Special Publication, vol. 76, pp. 405–416.